

1 **The significance of nitrogen regeneration for new production within a filament of the Mauritanian**  
2 **upwelling system.**

3  
4 D. R. Clark<sup>1</sup>, C. E. Widdicombe, A. P. Rees, E.M.S. Woodward.

5  
6 Plymouth Marine Laboratory, Prospect Place, West Hoe, Plymouth, PL1 3DH. United Kingdom.

7  
8 <sup>1</sup>Author for correspondence [drcl@pml.ac.uk](mailto:drcl@pml.ac.uk) Tel: (+44) 1752 633100

9  
10 **ABSTACT**

11 The Lagrangian progression of a biological community was followed in a filament of the Mauritanian  
12 upwelling system, North West Africa, during offshore advection. Inert dual tracers sulphur hexafluoride  
13 and helium-3 labelled a freshly upwelled patch of water that was mapped for 8 days. Changes in  
14 biological, physical and chemical characteristics were measured including phytoplankton productivity,  
15 nitrogen assimilation and regeneration. Freshly upwelled water contained high nutrient concentrations  
16 but was depleted in N compared to Redfield stoichiometry. The highest rate of primary productivity was  
17 measured on the continental shelf, associated with high rates of nitrogen assimilation and a  
18 phytoplankton community dominated by diatoms and flagellates. Indicators of phytoplankton  
19 abundance and activity decreased as the labelled water mass transited the continental shelf slope into  
20 deeper water, possibly linked to the mixed layer depth exceeding the light penetration depth. By the  
21 end of the study, primary productivity rate decreased and was associated with lower rates of nitrogen  
22 assimilation and lower nutrient concentrations. Nitrogen regeneration and assimilation took place  
23 simultaneously. Results highlighted the importance of regenerated  $\text{NH}_4^+$  in sustaining phytoplankton  
24 productivity and indicate that the upwelled  $\text{NO}_3^-$  pool contained an increasing fraction of regenerated  
25  $\text{NO}_3^-$  as it advected offshore. By calculating this fraction and incorporating it into an f-ratio formulation  
26 we estimated that of the 12.38 TgC of annual regional production, 4.73 TgC was exportable.

27  
28 **1. Introduction**

29 The combination of northeast trade winds and the Coriolis effect due to earth's rotation drives the  
30 upwelling of deep nutrient-rich waters into the photic zone of coastal regions in eastern ocean  
31 boundaries. Upwelling supports characteristically enhanced biological production and valuable  
32 ecosystem services typified by fisheries (Pauly and Christensen, 1995; Arístegui et al., 2009). The  
33 maturation and development of biological communities within upwelled water masses as they advect  
34 offshore reflects a characteristic feature of eastern boundary upwelling ecosystems (EBUE); the spatial  
35 separation of nutrient sources and sinks. Gauging the extent of biological production ultimately  
36 exported from upwelling regions is an area of continuing investigation and model development (Álvarez-  
37 Salgado et al., 2007; Arístegui et al., 2009).

38 The North West African upwelling system is possibly the least studied of the four global EBUE's  
39 (California, Peru-Chile, Iberia/North West Africa, Benguela) and is potentially the most complex due to  
40 its topography and circulation (Mittelstaedt, 1991; Tomczak and Godfrey, 2003; Arístegui et al., 2006,  
41 Chavez and Messié, 2009; Meunier et al., 2012). The Mauritanian region within this system is

1 characterised by a relatively wide shelf area over which upwelled water influences biological  
2 productivity (Mittelstaedt, 1991), while extended filaments and island induced eddies are additional  
3 features (Aristegui et al., 2009). The system can be separated into two regimes; the region between  
4 15°N and 20°N undergoes periodic upwelling which dominates during winter and spring, whereas the  
5 region north of 20°N is characterised by year round coastal upwelling with maximum intensity during  
6 summer and autumn (Mittelstaedt, 1991). The study region, located between 20-22°N, lies at the  
7 confluence between the two source waters upwelled in this system (North Atlantic Central Water and  
8 South Atlantic Central Water; Mittelstaedt, 1991), which differ in their salinity, temperature and  
9 nutrient characteristics. Nutrient concentrations and potential rates of new production in this region are  
10 towards the upper limits of the range reported for global EBUEs (Chavez and Messié, 2009).

11 The highly dynamic nature of upwelling systems challenges our ability to understand how biological  
12 activity develops as water masses advect offshore, and what the implications of this activity are for C-  
13 export. Both Eulerian (occupying a fixed location over time through which upwelled water passes) and  
14 Lagrangian (occupying a water mass as it passes through space and time) strategies have been adopted.  
15 The Eulerian approach was successfully applied in a study of the Northern Benguela by Postel et al.  
16 (2014); a challenge facing this approach is the risk that stations do not sample successive changes in  
17 upwelled water due to the dynamic meandering nature of advective transport. Drifting buoys have been  
18 used in previous Lagrangian studies of upwelling regions (Joint et al., 2001b; Wilkerson and Dugdale,  
19 1987) although buoy tracks diverge over time (D'Asaro, 2004) leading to uncertainty about the location  
20 of upwelled water masses. To address some of these issues in the present study, the inert gases sulphur  
21 hexafluoride (SF<sub>6</sub>) and helium-3 (<sup>3</sup>He) were used to label a water body within a recently upwelled  
22 filament (Nightingale et al., 2000). In combination with drifting buoys and mapping exercises, the  
23 progression of this labelled water mass and its associated biological activity was followed in Lagrangian  
24 mode during offshore advection. Our objective was to investigate phytoplankton productivity, microbial  
25 nitrogen cycling and to estimate exportable new production.

26 The assimilation of nitrogen by phytoplankton was introduced as a means of estimating 'new',  
27 'regenerated' and 'exportable' production (f-ratio; Dugdale and Goering, 1967; Eppley and Peterson,  
28 1979), based on the assumption that NO<sub>3</sub><sup>-</sup> regeneration and assimilation processes were spatially  
29 distinct, being associated with the aphotic and photic zones respectively. Consequently, the physical  
30 introduction of new nitrogen to the photic zone was deemed capable of supporting an increase in  
31 phytoplankton productivity which was available for export. This was readily measured as NO<sub>3</sub><sup>-</sup>  
32 assimilation, though included nitrogen derived from nitrogen fixation. All other forms of nitrogen were  
33 deemed to be regenerated, having previously been subject to microbial activity and capable only of  
34 sustaining rather than enhancing phytoplankton growth. This was readily measured as NH<sub>4</sub><sup>+</sup> assimilation,  
35 though included dissolved organic nitrogen (DON) forms. According to this concept, upwelling regions,  
36 which characteristically introduced deep nutrient rich waters to the photic zone, were associated with  
37 high f-ratios (i.e. >0.7) reflecting the high proportion of total nitrogen assimilation supported by NO<sub>3</sub><sup>-</sup>. By  
38 contrast, strong stratification in oligotrophic gyres suppressed nutrient inputs to the photic zone and  
39 biological competition for limited nutrient resources maintained very low NO<sub>3</sub><sup>-</sup> concentrations and f-  
40 ratios (i.e. <0.1).

1 Following the introduction of the new production paradigm it has been acknowledged that additional  
2 sources and processes related to the biogeochemical cycling of nitrogen are important to new  
3 production. Atmospheric inputs of nitrogen in oxidised, reduced and organic forms are significant for  
4 oceanic productivity (Baker et al., 2003; Moore et al., 2013; Powell et al., 2015). The nitrogen inventory  
5 of regions such as the North Atlantic is also influenced indirectly by atmospheric inputs, as iron  
6 associated with Saharan dust enhances diazotrophic nitrogen fixation, a source of new nitrogen to the  
7 surface ocean (Moore et al., 2009; Jickells and Moore, 2015). Although regenerated productivity has  
8 often been represented by, and measured as,  $\text{NH}_4^+$  assimilation, the significance of dissolved organic  
9 nitrogen (DON) as a substrate for primary producers has become clearer, including the assimilation of  
10 urea and amino acids (Bronk and Glibert, 1993; Bronk and Ward, 1999; Wafar et al., 2004; Moschonas et  
11 al., 2015). However, the contribution to total production (i.e. the sum of 'new' and 'regenerated'  
12 production) provided by organic forms of nitrogen are rarely considered in f-ratio calculations. A related  
13 issue is the active release of DON following inorganic nitrogen assimilation; by being released from  
14 phytoplankton cells rather than contributing to the formation of new cellular material (i.e. particulate  
15 organic nitrogen; PON), this nitrogen is removed from the dissolved inorganic nitrogen pool but is not  
16 incorporated into the measured rate of nitrogen assimilation using  $^{15}\text{N}$  techniques (Bronk et al., 1994;  
17 Raimbault and Garcia, 2008). Variability in the extent of DON release introduces error in the  $^{15}\text{N}$  budgets  
18 of tracer studies.

19 Error in measured rates of nitrogen assimilation is also introduced by concomitant processes which  
20 regenerate nitrogen (Glibert et al., 1982; Kanda et al., 1987).  $^{15}\text{NH}_4^+$  isotope dilution due to  $\text{NH}_4^+$   
21 regeneration was acknowledged in the new production paradigm while  $^{15}\text{NO}_3^-$  isotope dilution due to  
22 nitrification, the sequential oxidation of  $\text{NH}_4^+$  to  $\text{NO}_2^-$  to  $\text{NO}_3^-$  by nitrifying microbes, was assumed to be  
23 negligible within the photic zone (Dugdale and Goering, 1967). It has become clear that the process of  
24  $\text{NH}_4^+$  regeneration in upwelling systems is highly significant (Raimbault and Garcia, 2008; Clark et al.,  
25 2011; Fernández and Farías, 2012; Benavides et al., 2014); while zooplankton excretion and bacterial  
26 remineralisation are important sources of  $\text{NH}_4^+$ , mixotrophic nutrition may be a dominant strategy for  
27 the plankton community in upwelling systems, which contribute to  $\text{NH}_4^+$  regeneration (Benavides et al.,  
28 2014; Mitra et al., 2014). A recently acknowledged role may also exist for the photochemical  
29 degradation of DON which regenerates  $\text{NH}_4^+$  within the sunlit ocean (Rain-Franco et al., 2014). The  
30 combined influence of these processes provides a regenerative  $\text{NH}_4^+$  flux which can equal or exceed sink  
31 terms leading to sporadic  $\text{NH}_4^+$  accumulation (Fernández and Farías, 2012). Consequently, the influence  
32 of  $\text{NH}_4^+$  regeneration upon isotope dilution needs to be accounted for in  $\text{NH}_4^+$  assimilation rate  
33 measurements and subsequent f-ratio calculations.

34 The inhibition of nitrification by light supported the assumption that nitrification was not an  
35 important factor in f-ratio formulations for the photic zone (Olson, 1981). Although subsequent studies  
36 have supported this distribution in nitrifying activity, measurements have demonstrated that  $\text{NO}_3^-$   
37 regeneration is significant when compared to concurrent  $\text{NO}_3^-$  assimilation in the photic zone  
38 (Fernández et al., 2005, 2009; Fernández and Farías, 2012; Clark et al., 2011; 2014). Consequently,  
39 although isotope dilution due to the regeneration of  $\text{NO}_3^-$  can be accounted for in  $\text{NO}_3^-$  assimilation rate  
40 calculations, it is implicit that the surface ocean  $\text{NO}_3^-$  pool contains a fraction of regenerated  $\text{NO}_3^-$  which  
41 cannot readily be measured directly (Martin and Pondaven, 2006).

1 Conceptually, improving the utility of f-ratio measurements would require a full consideration of all  
2 new and regenerated forms of inorganic nitrogen to the photic zone which support primary  
3 productivity. However, uncertainty about the fraction of photic zone  $\text{NO}_3^-$  that truly represents 'new'  
4  $\text{NO}_3^-$  is an important and conceptually fundamental limitation that has rarely been acknowledged.  
5 Upwelling areas are an exceptional case; seawater upwelled in the Mauritanian system may be regarded  
6 as genuinely 'new' to the photic zone, consistent with the original concept. Here we aimed to examine  
7 the concept of a transition in  $\text{NO}_3^-$  pool provenance from 'new' towards 'regenerated' and to investigate  
8 the implications for exportable production estimates in the Mauritanian Upwelling system.

## 9 10 **2. Materials and methods**

11 The study was undertaken on board the RRS Discovery (D338; 15<sup>th</sup> April to 27<sup>th</sup> May 2009) as a UK  
12 contribution to the international Surface Ocean Lower Atmosphere Study (SOLAS) project. Remotely  
13 sensed data was processed by NEODAAS at PML and used to identify a region of active upwelling.  
14 Chlorophyll 'a' data was received by NASA from MODIS and processed using the OC3 chlorophyll  
15 algorithm in NASA's SeaWiFS software. Sea-surface temperature data was received by NOAA from  
16 AVHRR and were processed using PML's in-house Panorama processing system (Miller et al., 1997).  
17 Upwelling activity was confirmed by hydrographical surveys of water column physical structure involving  
18 CTD rosette casts, Moving Vessel Profiler (MVP; incorporating CTD and fluorescence units) deployments  
19 and the use of a shipboard Acoustic Doppler Current Profiler (ADCP; for full details of the mapping  
20 exercise see Meunier et al., 2012). This data was used to select the position for drifter buoy deployment.  
21  $\text{SF}_6/{}^3\text{He}$  was deployed in a patch (hereafter referred to as  $P_1$ ) at a depth of 5m around the drifter; full  
22 details of the dual tracer technique used during this research program are described in Nightingale et al.  
23 (2000). The time interval between receiving satellite data and deploying  $\text{SF}_6/{}^3\text{He}$  was < 2 days.

24  $\text{SF}_6/{}^3\text{He}$  was subsequently detected using two ship-based Gas Chromatography (GC) systems.  
25 Seawater samples were collected in discrete mode from depth profiles using CTD rosette-mounted  
26 Niskin bottles and continuous mode from the ships seawater supply collected at approximately 5m. This  
27 analysis identified changes in the horizontal and vertical distribution of  $\text{SF}_6/{}^3\text{He}$  marked seawater. It  
28 ensured that seawater sampling for observational measurements was centred upon the labelled water  
29 mass and that the same water mass was sampled until tracer concentrations could no longer be  
30 detected reliably, due to the limits of detection associated with GC analysis. Using this approach,  
31 chemical, physical and biological characteristics of the water mass were measured in Lagrangian mode.  
32 The duration of the study was 8 days, with sequential sampling days identified by the notation  $T_0$ - $T_7$ ;  
33 pre-patch observations are referred to as  $T_{-1}$ . One day of sampling was lost due to challenging weather  
34 conditions ( $T_5$ , 28<sup>th</sup> April).

35 For nitrogen regeneration ( $\text{NH}_4^+$  regeneration,  $\text{NH}_4^+$  oxidation,  $\text{NO}_2^-$  oxidation) and nitrogen  
36 assimilation ( $\text{NH}_4^+$ ,  $\text{NO}_2^-$  and  $\text{NO}_3^-$ ) process measurements, seawater samples were collected from CTD  
37 rosette-mounted Niskin bottles which sampled routinely at a depth equivalent to 55% of surface  
38 photosynthetically active radiation (sPAR). Additional samples were taken from the 1% sPAR depth for  
39  $\text{NO}_2^-$  oxidation rate measurements only.

40 The assimilation and regeneration of DIN was investigated using  ${}^{15}\text{N}$  amended seawater during deck  
41 incubations (Clark et al., 2014). Simultaneously, size fractionated primary productivity was measured in

1 depth profiles using deck incubations with  $^{14}\text{C}$  (Tilstone et al., 2009). For all deck incubations, neutral  
2 density filters simulated sPAR according to Joint Global Ocean Flux Study protocols (Intergovernmental  
3 Oceanographic Commission, 1994) and temperature control was achieved by flushing boxes with  
4 seawater from the ships sea-surface supply collected at approximately 5m.

## 5 6 2.1 Nitrogen regeneration investigations.

7 A 24-position stainless steel rosette system was used to collect seawater from specific depths using  
8 20 L Niskin bottles. Water columns were characterised during casts using additional instrumentation  
9 attached to the rosette, which included Seabird 9 Plus conductivity, temperature, depth (CTD) units, a  
10 Seabird SBE 43 dissolved oxygen sensor and a Chelsea MKIII Aquatracka fluorometer. Seawater was  
11 collected during pre-dawn casts (approximately 04:00) at depths equivalent to specific sPAR values,  
12 which were derived from the previous days light attenuation profiles. All glassware used for the  
13 manipulation of seawater was cleaned with 10 % HCL (reagent grade, 37 %) between CTD sampling  
14 iterations and rinsed thoroughly with Milli-Q high purity water within sampling iterations. Chemicals and  
15 solvents were analytical and High Performance Liquid Chromatography (HPLC) grade respectively,  
16 supplied by Sigma-Aldrich (UK) unless otherwise stated. Stable isotope salts ( $^{15}\text{NH}_4\text{Cl}$ ,  $\text{Na}^{15}\text{NO}_3$ ,  $\text{Na}^{15}\text{NO}_2$ )  
17 were supplied by CK gas products Ltd (UK).

18 A 20 L volume of seawater from each sampling depth was collected in a blacked-out Nalgene  
19 container. In the ships laboratory, the preparation of this seawater for incubation studies was also  
20 undertaken using blacked-out containers to minimise sample exposure to artificial light sources and the  
21 potential disruption of the biological community's natural light-dark cycle. Collected seawater was not  
22 pre-filtered (i.e. to remove particles greater than a specific size). As an overview, 6 L of this seawater  
23 was used for nitrogen assimilation studies while 12 L was used for nitrogen regeneration studies.  
24 Generally, nitrogen regeneration studies were initiated prior to 09:00 GMT and terminated prior to  
25 17:00 GMT providing an average incubation time of 8 hours. Within this incubation period, nitrogen  
26 assimilation studies were generally initiated by 10:00 GMT and terminated by 16:00 GMT providing an  
27 average incubation time of 6 hours. Incubations were therefore restricted to day-light hours.

28  $\text{NH}_4^+$  regeneration rate was determined by amending a 4 L volume of seawater in a blacked out  
29 container with  $^{15}\text{NH}_4^+$ , achieving an average enrichment of  $10.7\pm 8.4\%$   $^{15}\text{NH}_4^+$ . This volume was  
30 thoroughly mixed and left to stand for 20 minutes in order to ensure homogeneity. Amended seawater  
31 was used to fill a 2.2 L incubation bottle, which was placed in a deck incubator at simulated light and  
32 temperature. The remaining amended seawater was filtered through GF/F glass fibre filters and  
33 triplicate 100 mL volumes were set aside for the determination of pre-incubation  $\text{NH}_4^+$  concentration  
34 and isotopic enrichment by synthesising indophenol as described below. Following the deck incubation,  
35 bottle contents were filtered through GF/F filters and the filtrate was distributed between 3 x 100 mL  
36 volumes for the determination of post-incubation  $\text{NH}_4^+$  concentration and isotopic enrichment by  
37 synthesising indophenol.

38 A comparable procedure was used for  $\text{NH}_4^+$  and  $\text{NO}_2^-$  oxidation incubations in which separate 4 L  
39 volumes of seawater were amended with  $^{15}\text{NO}_2^-$  and  $^{15}\text{NO}_3^-$ , achieving average  $^{15}\text{N}$  enrichments of  
40  $8.8\pm 0.9\%$  and  $9.4\pm 0.9\%$  respectively. The concentration and isotopic enrichment of  $\text{NO}_2^-$  was  
41 determined by synthesising sudan-1 in sample volumes of 100 mL, as described below. The

1 concentration and isotopic enrichment of  $\text{NO}_3^-$  was determined by first reducing  $\text{NO}_3^-$  to  $\text{NO}_2^-$  using a  
2 high capacity cadmium column, and then synthesising sudan-1 in volumes of 25-50 mL varying with  
3 ambient concentration.

4 Indophenol was synthesised in samples by adding the first reagent (4.7 g phenol and 0.32 g sodium  
5 nitroprusside in 200 mL Milli Q water) in the proportion of 1 mL per 100 mL of sample volume, mixing  
6 the sample and leaving for 5 minutes. The second reagent (1.2 g sodium dichloro-isocyanurate and 2.8 g  
7 sodium hydroxide in 200 mL Milli Q) was then added in the proportion of 1 mL per 100 mL sample  
8 volume, mixed and left for 8 hours at room temperature for indophenol development. Indophenol was  
9 collected by solid-phase extraction (SPE). Sudan-1 was synthesised by adding the first reagent (0.8 g of  
10 aniline sulphate in 200 mL 3M HCl) to samples in the proportion 0.5 mL per 100 mL sample volume.  
11 Samples were mixed and left for 5 minutes to homogenise after which sample pH was verified to be  
12 approximately 2.0. Reagent 2 (24 g NaOH and 0.416 g 2-naphthol in 200 mL Milli Q) was added in the  
13 proportion 0.5 mL per 100 mL sample volume. Samples were again mixed, left for 5 minutes before  
14 sample pH was verified to be approximately 8.0. Sudan-1, the development of which was complete after  
15 30 minutes of incubation at room temperature, was collected by SPE.

16 Deuterated internal standards were added to samples immediately prior to SPE collection.  
17 Deuterated indophenol and deuterated sudan-1 were synthesised according to methods described  
18 previously (Clark et al., 2006; 2007) and purified by HPLC. Standard solutions in methanol were prepared  
19 ( $100 \text{ ng}\cdot\mu\text{L}^{-1}$ ) and the concentration verified against analytical standard solutions (Sigma-Aldrich).  
20 Appropriate volumes of deuterated internal standards (i.e. comparable to sample size) were added to  
21 samples following acidification by citric acid and prior to SPE collection.

22 Indophenol and sudan-1 were collected by SPE using 6 mL/500 mg C18 cartridges (Biotage, UK)  
23 which were prepared for sample collection by first rinsing with 5 mL methanol, followed by 5 mL Milli Q  
24 water and 5 mL 0.22  $\mu\text{m}$  filtered seawater. Prior to sample collection seawater samples were acidified  
25 with 1 M citric acid to a pH of 5.5, before collection by SPE under low vacuum (120 mmHg) at a flow rate  
26 of approximately 1 mL per minute without drying. Samples were then rinsed with 5 mL 0.22  $\mu\text{m}$  filtered  
27 seawater and 5 mL Milli Q water before being air dried under high vacuum (360 mmHg). Samples were  
28 stored frozen until further processing at the land based laboratory.

29 At the land based laboratory, samples were brought to room temperature and prepared for HPLC  
30 purification and Gas Chromatography Mass Spectrometry (GCMS) analysis in the following way.  
31 Indophenol samples were eluted from SPE cartridges in 2 mL methanol. Samples were placed in a  
32 bench-top centrifuge for 2 minutes at 20 000xG to remove particulate material derived from the SPE  
33 column. A 500  $\mu\text{L}$  sub-sample was used for HPLC purification and GCMS analysis and the remaining 1.5  
34 mL was stored at  $-20^\circ\text{C}$  for any subsequent repetition of the analysis. 500  $\mu\text{L}$  sub-samples were  
35 evaporated under oxygen-free nitrogen (OFN) to 200  $\mu\text{L}$  for HPLC, during which it was essential that  
36 samples were not reduced to dryness. 175  $\mu\text{L}$  of the 200  $\mu\text{L}$  samples were purified by HPLC using the  
37 preparative system, mobile phases and profile described in Clark et al. (2006) in combination with a  
38 Gemini-NX 5u C18 110A 250 x 4.6 mm column (Phenomenex, UK) with sample peak collection at a  
39 retention time of 38-40 minutes. Collected sample fractions were blown dry under OFN at room  
40 temperature. Dried samples were stored for > 24 hours over anhydrous silica gel at room temperature  
41 prior to GCMS analysis. Samples were derivitised in 50  $\mu\text{L}$  of 2.5 % Sylon HT in n-hexane and incubated

1 at 50 °C for 4 hours. Samples were analysed by GCMS using the system, ramping profiles and extracted  
 2 ions described in Clark et al. (2006). Internal standards were used to quantify sample  $\text{NH}_4^+$   
 3 concentration, and when combined with sample enrichment, the rate of  $\text{NH}_4^+$  regeneration was  
 4 determined by applying the Blackburn-Caperon model (Blackburn, 1979; Caperon et al., 1979).

5 SPE columns loaded with sudan-1 samples were brought to room temperature and processed for  
 6 HPLC purification and GCMS analysis in the following way. Sudan-1 samples were eluted from SPE  
 7 cartridges in 2 mL of ethyl acetate. 100-300  $\mu\text{L}$  sub-samples were used for further processing while the  
 8 remaining samples were stored at -20 °C and available for subsequent repeated analysis. 100-300  $\mu\text{L}$   
 9 sub-samples were blown dry under OFN, re-dissolved in 200  $\mu\text{L}$  methanol and centrifuged in a bench-  
 10 top unit at 20 000xG for 2 minutes to remove particulate material derived from the SPE packing.  
 11 Samples were transferred to GC vials and purified by HPLC. The HPLC system described in Clark et al.  
 12 (2007) was used in combination with the Gemini column identified above and the mobile phase profile  
 13 described in Clark et al. (2014). Sample fractions, which were collected at retention time 25.5-27.5  
 14 minutes, were dried using a Zymark Turbovap evaporation unit at 50 °C using OFN. Dried samples were  
 15 transferred to GC vials and stored over anhydrous silica gel for 24 hours prior to derivitisation in a 50  $\mu\text{L}$   
 16 volume of 2.5 % MTBSTFA in ethyl acetate at 70 °C for 2 hours. The GCMS unit, ramping profile and  
 17 extracted ions described in Clark et al. (2007) were used to derive sample  $\text{NO}_2^-/\text{NO}_3^-$  concentration and  
 18 isotopic enrichment. The rate of  $\text{NH}_4^+$  or  $\text{NO}_2^-$  oxidation was derived by re-arranging the mixing model of  
 19 Sweeney et al. (1978) as described in Clark et al. (2007) and by applying the Blackburn-Caperon model  
 20 (Blackburn, 1979; Caperon et al., 1979).

## 22 2.2 Nitrogen assimilation measurements and the f-ratio.

23 Using 6 L of seawater, nitrogen assimilation rates were derived using  $^{15}\text{N}$  techniques. Triplicate  
 24 660 mL volumes of seawater were separately amended with  $^{15}\text{NH}_4^+$  and  $^{15}\text{NO}_3^-$  at an enrichment of  
 25  $7.8 \pm 1.8\%$  and  $8.0 \pm 1.7\%$  of the ambient concentration respectively. Bottles were placed in deck  
 26 incubators in conditions of simulated in-situ light and temperature. A volume of un-amended seawater  
 27 was filtered through GF/F and used to derive the  $^{15}\text{N}$  natural abundance in particulate matter. Deck  
 28 incubations were terminated by filtration onto GF/F filters, which were frozen at -20 °C until isotope  
 29 ratio mass spectrometry analysis was undertaken at the land based laboratory. The rates of nitrogen  
 30 assimilation ( $\rho\text{NH}_4^+$ ,  $\rho\text{NO}_3^-$ ) were determined using the equations of Dugdale and Goering (1967),  
 31 corrected for nitrogen regeneration using the equations of Kanda et al. (1987).

32 Nitrogen assimilation data (not corrected for isotope dilution) was used to derive f-ratio values by  
 33 the original formulation as;

$$f - ratio = \frac{\rho\text{NO}_3^-}{\rho\text{NO}_3^- + \rho\text{NH}_4^+}$$

34 The f-ratio was re-calculated using nitrogen assimilation rate data corrected for isotope dilution ( $f_c$ -  
 35 ratio). An additional formulation ( $f_{\text{regen}}$ -ratio) calculated the f-ratio by including a consideration of  
 36 previously regenerated  $\text{NO}_3^-$  within  $P_1$ , represented as the fraction of the total  $\text{NO}_3^-$  pool remaining as  
 37 new  $\text{NO}_3^-$  ( $R_{\text{NO}_3}$ );

$$f_{\text{regen}} - ratio = \frac{(\rho\text{NO}_3^- \cdot R_{\text{NO}_3})}{((\rho\text{NO}_3^- \cdot R_{\text{NO}_3}) + \rho\text{NH}_4^+)}$$

1 The term  $R_{\text{NO}_3}$  was calculated using the following procedure and assumptions; it was assumed that  
2  $R_{\text{NO}_3}$  was conserved (i.e. no mixing took place); that  $\text{NO}_3^-$  assimilation was restricted to a 12 hour light  
3 phase; that phytoplankton did not differentiate between 'new' and 'regenerated'  $\text{NO}_3^-$ ; that the  
4 measured rate of  $\text{NO}_2^-$  oxidation (which regenerates  $\text{NO}_3^-$ ) was sustained for each 24 hour iteration. As  
5 an indication of the utility of using  $\text{NO}_3^-$  assimilation and regeneration processes to reflect  $\text{NO}_3^-$  pool  
6 turnover, a variance of up to  $\pm 25\%$  in calculated compared to measured  $\text{NO}_3^-$  pool concentration was  
7 measured on a daily basis. However, over the duration of the study ( $T_{-1}$ - $T_7$ ) this difference was  $-0.2\%$ ,  
8 indicating that changes in ambient  $\text{NO}_3^-$  concentration was adequately described by considering only  
9 these processes within the constraints stated.

10 Using  $T_{-1}$  as an example, the ambient pool was assumed to have a  $R_{\text{NO}_3}$  value of 1, indicating that it  
11 was composed of 'new'  $\text{NO}_3^-$  only. The amount of  $\text{NO}_3^-$  regenerated in this 24 h period was calculated  
12 and added to the ambient concentration. The value of  $R_{\text{NO}_3}$  after this 24 hour period was calculated by  
13 dividing the ambient pool concentration (all new  $\text{NO}_3^-$  for this first time point) by the sum of ambient  
14 and regenerated  $\text{NO}_3^-$  to give a value of 0.94. For the next 24 hour period ( $T_0$ ), the concentration of  
15 'new'  $\text{NO}_3^-$  was calculated by multiplying the  $T_0$  ambient  $\text{NO}_3^-$  concentration by the  $T_{-1}$   $R_{\text{NO}_3}$  value. The  
16  $R_{\text{NO}_3}$  value at the end of this 24 hour period was calculated by dividing the concentration of new  $\text{NO}_3^-$  by  
17 the sum of ambient and newly regenerated (i.e. within  $T_0$ )  $\text{NO}_3^-$  to provide a value of 0.81. This process  
18 was repeated for the study period.

### 19 20 2.3 Primary productivity measurements

21 Phytoplankton productivity was measured using the  $^{14}\text{C}$  method (Tilstone et al., 2009). Samples were  
22 collected pre-dawn from 5 depths (97%, 55%, 33%, 14%, 1% sPAR). Triplicate 75 mL subsamples were  
23 amended with between 185 and 740 kBq (5–20  $\mu\text{Ci}$ )  $\text{NaH}^{14}\text{CO}_3$  and incubated on-deck for 24 hours at  
24 simulated sPAR depth. Incubations were terminated by sequential filtration through 2  $\mu\text{m}$  and 0.2  $\mu\text{m}$   
25 polycarbonate filters.  $^{14}\text{C}$  disintegration was measured on-board using a TriCarb liquid scintillation  
26 counter.

### 27 28 2.4 Chlorophyll concentration

29 Chlorophyll 'a' samples were collected simultaneously with seawater used for primary productivity  
30 measurements; 250mL subsamples were collected from 5 depths (97%, 55%, 33%, 14%, 1% sPAR) from  
31 pre-dawn CTD casts and immediately filtered sequentially through a 2  $\mu\text{m}$  and 0.2  $\mu\text{m}$  polycarbonate  
32 filters. Filters were soaked in 10 mL 90% acetone for 12 hours and extracts analysed fluorometrically  
33 using a Trilogy Turner fluorometer calibrated against pure chlorophyll 'a' standards (Sigma).

### 34 35 2.5 Microscopy

36 Seawater samples were collected from 5 depths (97%, 55%, 33%, 14%, 1% sPAR) during pre-dawn  
37 CTD casts. Samples were immediately fixed in acid-Lugol's iodine solution (2% final concentration).  
38 Where possible cells were identified to species-level according to the published literature and assigned  
39 to three functional groups (diatoms (centric & pennate), dinoflagellates, flagellates). Cells were  
40 enumerated and expressed as  $\text{cells}\cdot\text{mL}^{-1}$ .



## 1 2.6 Inorganic nutrients

2 Seawater samples were collected from a range of depths during pre-dawn CTD casts into cleaned,  
3 acid-washed, and 'aged' high density polyethylene sample bottles, using clean handling and analysis  
4 procedures. Samples were analyzed immediately. Nitrate, nitrite, ammonium, phosphate and silicate  
5 were measured colorimetrically with a 5-channel segmented flow Bran and Luebbe AAIII autoanalyzer,  
6 using methods described previously (Woodward and Rees, 2001).

## 8 3. Results and discussion

9 The inert dual tracers SF<sub>6</sub> and <sup>3</sup>He (Nightingale et al., 2000) in combination with drifter buoys were  
10 used in this study so that filament progression and biological community development could be  
11 followed in Lagrangian mode as the water mass advected offshore (Fig. 1). The loss of tracers to the  
12 atmosphere, their dilution due to mixing with unlabelled water and the detection limit of GC analysis  
13 constrained patch monitoring duration. A detailed description of filament dynamics forming off Cap  
14 Blanc during this study is presented in Meunier et al. (2012). Both North and South Atlantic Central  
15 Water (NACW and SACW respectively) is upwelled in this region and the contribution to filaments from  
16 each source can be distinguished; SACW generally contains higher nutrient concentrations and has  
17 higher temperature with lower oxygen and salinity. Optimum parameter analysis (Rees et al., 2011)  
18 demonstrated that the filament studied was dominated by NACW (50-80%).

19 P<sub>1</sub> was identified using a combination of near-real time remotely sensed data and water column  
20 profiling. Following identification, observational measurements were undertaken and SF<sub>6</sub>/<sup>3</sup>He tracers  
21 were deployed at a depth of 5m in a square spiral (1.0 x 0.8km) around a central drifting buoy. Tracers  
22 were detected throughout the surface Mixed Layer Depth (MLD) of 50 m within 1 day of deployment.  
23 Extensive mapping exercises were conducted to describe P<sub>1</sub>'s progression as the water mass advected  
24 offshore in a south-westerly then westerly direction. Mapping enabled the patch centre to be located  
25 for daily observational measurements. During this study, P<sub>1</sub> remained tightly constrained for the first 3  
26 days until the patch left the continental shelf area and entered the upper slope and shelf break regions.  
27 During this latter stage enhanced vertical mixing due to increased water column depth combined with  
28 horizontal shear associated with patch proximity to the northern edge of the filament lead to P<sub>1</sub>  
29 elongation and dispersion.

### 31 3.1 Description of the physical and chemical regime.

32 Selected chemical, biological and physical characteristics of the water column are presented in Fig.  
33 1-4. As P<sub>1</sub> advected offshore its temperature increased from approximately 16.4 °C on T<sub>-1</sub> to >17.6 °C by  
34 T<sub>7</sub> (Fig 1). Profiles of water column temperature demonstrated changes in vertical structure as the mixed  
35 layer depth increased from approximately 50m (T<sub>-1</sub> – T<sub>2</sub>) to 100m coinciding with the continental shelf to  
36 shelf break transition (T<sub>3</sub>, Loucaides et al., 2012). Nutrient concentrations in P<sub>1</sub> were greatest during the  
37 first day of Lagrangian study and then progressively decreased (with the exception of NO<sub>2</sub><sup>-</sup>; Fig. 2). On  
38 average, NO<sub>3</sub><sup>-</sup> concentration decreased from 9.0±0.1 μmol·L<sup>-1</sup> to 4.6±0.3 μmol·L<sup>-1</sup>, Si concentration  
39 decreased from 2.7±0.1 μmol·L<sup>-1</sup> to 0.9±0.1 μmol·L<sup>-1</sup> and PO<sub>4</sub><sup>3-</sup> concentration decreased from 0.7±0.1  
40 μmol·L<sup>-1</sup> to 0.4±0.1 μmol·L<sup>-1</sup>. The greatest decrease in nutrient concentrations occurred on the  
41 continental shelf. Following advection over the shelf break, these nutrient concentrations continued to

1 decrease albeit at a lower rate. By contrast,  $\text{NO}_2^-$  concentration remained relatively stable for the  
2 duration of the study at  $0.31 \pm 0.05 \mu\text{mol}\cdot\text{L}^{-1}$  while a simple increasing or decreasing trend in  $\text{NH}_4^+$   
3 concentration was not evident; an average value of  $0.8 \pm 0.23 \mu\text{mol}\cdot\text{L}^{-1}$  was measured.

4 Nutrient stoichiometry of the upwelled  $P_1$  water mass (i.e. within the upper mixed layer) indicated  
5 nitrogen deficiency (Fig. 3); regression provided a N:P value of 13.9:1 compared to a value of 17.7:1  
6 below the mixed layer (incorporating depths up to 1400 m). This value for the photic zone is consistent  
7 with the range of 10-16 reported for freshly upwelled coastal waters by Zindler et al. (2012) in their  
8 study of the Mauritanian upwelling. The difference in N:P values between depths i.e. for  $P_1$  within the  
9 upper mixed layer compared to depths below this, is likely to reflect the relatively rapid biological  
10 consumption of N relative to P within the photic zone (Zindler et al., 2012). In contrast, the Namibian  
11 shelf's mud belt is a region of continuous N loss and P efflux to the pelagic environment of the Benguela  
12 upwelling system, leading to characteristically low N:P ratios. Gregor and Monteiro (2013), who  
13 reported pelagic N:P values of 7.2-12.3, identified denitrification and sulphate reduction as anoxic  
14 benthic processes leading to this relative nitrogen deficiency, supported by Flohr et al. (2014).

15 The relative nitrogen deficiency measured in  $P_1$  implied a relative P-excess ( $P^*$ , calculated as  $[\text{PO}_4^{3-}] -$   
16  $([\text{NO}_3^-]/16)$ ). An average  $P^*$  of  $72 \pm 18 \text{ nmol}\cdot\text{L}^{-1}$  (Fig. 2f and 3) indicated that  $P_1$  exported phosphate to the  
17 adjacent oligotrophic gyre of the North Atlantic. The magnitude of this export was less than the value of  
18  $< 300 \text{ nmol}\cdot\text{L}^{-1}$  reported for phosphate advection to the South Atlantic gyre by the Benguela Upwelling  
19 System (Flohr et al., 2014). A  $P^*$  decline towards zero would be anticipated with offshore advection due  
20 to nitrogen fixation, supported by atmospheric dust associated iron inputs to the North Atlantic derived  
21 from the Sahara region. Dust inputs mitigate the enhanced iron requirements of nitrogen fixing  
22 diazotrophs (Moore et al., 2009), ultimately providing a new nitrogen source to the North Atlantic  
23 Ocean (Deutsch et al., 2007). In their study of the Benguela Upwelling region, Sohm et al. (2011)  
24 suggested that environmental conditions influencing nitrogen fixation are poorly understood and that  
25 nitrogen fixing activity extends beyond the tropical and sub-tropical low nutrient regions  
26 characteristically considered, to include cool, high nutrient regions. They reported nitrogen fixation  
27 rates approaching  $8 \text{ nmol}\cdot\text{L}^{-1}\cdot\text{d}^{-1}$ , potentially supported by sedimentary sources of iron during a period of  
28 low atmospheric dust input. In contrast, undetectable or low rates of nitrogen fixation ( $< 1 \text{ nmol}\cdot\text{L}^{-1}\cdot\text{d}^{-1}$ )  
29 in the Benguela have been reported to make an insignificant contribution to new production (Staal et  
30 al., 2007; Benavides et al., 2014; Wasmund et al., 2015). A comparable conclusion for freshly upwelled  
31 water was reached during the present study as nitrogen fixation rates in  $P_1$  were undetectable (Rees,  
32 unpubl).

33 Analysis demonstrated that nutrient drawdown during  $P_1$  progression was driven by biological  
34 processes (Loucaides et al., 2012); factors such as horizontal and vertical mixing with low nutrient water  
35 masses derived from outside of the upwelled filament were unlikely to have made a significant  
36 contribution. However, an entrainment event associated with increased mixed layer depth lead to a  
37 small but measurable recovery in nutrient concentrations during  $T_3$ - $T_4$ .

38 Nutrient drawdown supported high rates of primary production (Fig. 4). Rates were measured within  
39 the range  $0.1$ - $0.7 \text{ molC}\cdot\text{m}^{-2}\cdot\text{d}^{-1}$  which sets an upper limit for C-export through a combination of  
40 particulate material sedimentation (Nowald et al., 2015), lateral transport of dissolved organic matter  
41 (Álvarez-Salgado et al., 2007), and trophic transfer. The range in primary productivity was comparable to

1 the value of  $0.2 \text{ molC}\cdot\text{m}^{-2}\cdot\text{d}^{-1}$  reported for the region by Minas et al. (1986) and potentially exceeds that  
2 measured in other upwelling areas; values of  $0.02\text{-}0.21 \text{ molC}\cdot\text{m}^{-2}\cdot\text{d}^{-1}$  were reported for the Iberian  
3 upwelling (Joint et al., 2001a; Álvarez-Salgado et al., 2002; Arístegui et al., 2006),  $0.01\text{-}0.46 \text{ molC}\cdot\text{m}^{-2}\cdot\text{d}^{-1}$   
4 were reported for the Peruvian upwelling (Fernández et al., 2009), an average of  $0.23 \text{ molC}\cdot\text{m}^{-2}\cdot\text{d}^{-1}$  was  
5 reported for the Southern Benguela (Shannon and Field, 1985) and  $0.07 \text{ molC}\cdot\text{m}^{-2}\cdot\text{d}^{-1}$  was reported for  
6 the Californian Upwelling Ecosystem (Santoro et al., 2010).

7 In terms of distribution, the highest rates of primary productivity were associated with the  
8 continental shelf region ( $0.49\text{-}0.69 \text{ molC}\cdot\text{m}^{-2}\cdot\text{d}^{-1}$ ), with rates decreasing as  $P_1$  advected over the shelf  
9 break ( $0.11\text{-}0.25 \text{ molC}\cdot\text{m}^{-2}\cdot\text{d}^{-1}$ ). This distribution was characteristic of the coastal North West African  
10 region, with high biological productivity associated with the continental shelf area influenced by  
11 upwelling (Mittelstaedt, 1991; Arístegui et al., 2009).

### 12 13 3.2 Phytoplankton composition and nitrogen assimilation.

14 Freshly upwelled water is extremely low in chlorophyll content and productivity, and would  
15 characteristically contain a  $\text{NO}_3^-$  concentration in the range  $9\text{-}15 \mu\text{mol}\cdot\text{L}^{-1}$  for this region (Arístegui et al.,  
16 2009, noting that  $P_1$ 's composition of NACW and SACW would place freshly upwelled water towards the  
17 upper end of this range). Consequently, productivity had become established and decreased  $\text{NO}_3^-$  by up  
18 to  $6 \mu\text{mol}\cdot\text{L}^{-1}$  prior to this study which followed the removal of a further  $4 \mu\text{mol}\cdot\text{L}^{-1}$  of  $\text{NO}_3^-$ . During  $P_1$   
19 progression, clear transitions in phytoplankton abundance, nitrogen biomass and nitrogen assimilation  
20 activity took place (Fig. 5). The highest abundance of all phytoplankton was measured during the first 3  
21 days of Lagrangian study ( $T_0\text{-}T_2$ ). Although flagellates were numerically dominant, diatoms dominated  
22 carbon biomass representing between 40-80% (data not shown). Cell abundance decreased beyond  $T_2$   
23 although specific phytoplankton classes represented a consistent proportion of total abundance  
24 suggesting that selective removal was not an important factor; for the duration of this study, diatoms  
25 represented  $12.7\pm 5.7\%$ , dinoflagellates represented  $0.10\pm 0.02\%$ , flagellates represented  $87.2\pm 5.7\%$  of  
26 total cell abundance. The trend of progressively diminishing phytoplankton abundance was reflected in  
27 the concentration of PON which decreased by 75% within 8 days.

28 During this study,  $\text{NH}_4^+$  assimilation was measured within the range  $6.1\text{-}32.8 \text{ nmol}\cdot\text{L}^{-1}\cdot\text{h}^{-1}$ , while  $\text{NO}_3^-$   
29 assimilation was measured within the range  $3.9\text{-}43.8 \text{ nmol}\cdot\text{L}^{-1}\cdot\text{h}^{-1}$ . There are relatively few studies of  
30 nitrogen assimilation in the North West African region against which to draw comparisons;  $\text{NO}_3^-$   
31 assimilation measured within the photic zone was previously reported in the range  $<0.2\text{-}31 \text{ nmol}\cdot\text{L}^{-1}\cdot\text{h}^{-1}$   
32 (Varela et al., 2005; Dugdale et al., 1990) while  $\text{NH}_4^+$  assimilation was reported in the range  $<0.2\text{-}105$   
33  $\text{ nmol}\cdot\text{L}^{-1}\cdot\text{h}^{-1}$  (Varela et al., 2005; Benavides et al., 2013). The fact that rates of  $\text{NH}_4^+$  and  $\text{NO}_3^-$  assimilation  
34 were broadly similar for  $P_1$  despite the difference in nitrogen source availability was perhaps the most  
35 striking observation. The average  $P_1$   $\text{NH}_4^+$  and  $\text{NO}_3^-$  concentrations were  $0.80\pm 0.23 \mu\text{mol}\cdot\text{L}^{-1}$  and  
36  $6.22\pm 1.20 \mu\text{mol}\cdot\text{L}^{-1}$  respectively, differing by almost one order of magnitude. Results underscore the  
37 importance of regenerated nitrogen in supporting phytoplankton nitrogen requirements even from the  
38 early stages of upwelling and imply that this form of inorganic nitrogen was rapidly recycled. The  
39 significance of nitrogen regeneration in upwelling regions has previously been highlighted (Raimbault  
40 and Garcia, 2008; Clark et al., 2011; Fernández and Farías, 2012; Benavides et al., 2014).

1 Within the conveyor belt scheme describing productivity cycles in upwelling systems (Wilkerson and  
2 Dugdale, 2008), the increase of phytoplankton growth in response to favourable light and nutrient  
3 conditions (shift-up phase) is followed by a shift-down phase driven by factors such as sedimentation  
4 and grazing. Cycles last between five and seven days. The trend of progressively diminishing indicators  
5 of phytoplankton abundance and activity in combination with a calculated residence time within the  
6 photic zone of 3 days for upwelled water prior to  $T_0$  (Meunier et al., 2012; Loucaides et al., 2012)  
7 suggested that the peak and shift-down stages of phytoplankton productivity were investigated here.  
8 Contributory factors (excluding sedimentation and grazing for which we have no data) to the shift-down  
9 phase are discussed below.

10 In previous studies of upwelling regimes, inorganic nutrient availability has been identified as a  
11 limiting resource driving changes in community structure and productivity (Wilkerson and Dugdale,  
12 2008). Nutrient limitation of larger cells, which dominated productivity in the present study, may have  
13 been a contributory factor. For example, the average N:Si ratio for the duration of  $P_1$  ( $4.49 \pm 0.78$ )  
14 indicated potential silicate limitation of diatom growth (Brzezinski, 1985; Gilpin et al., 2004). However,  
15 relatively high nutrient concentrations were detected by  $T_7$  and a shift in community structure was not  
16 observed; the comparable decrease in cell abundance across all phytoplankton classes implied a less  
17 specific driver behind the decrease in biomass during the relatively short duration of this investigation.

18 Light may be considered as a limiting resource; profiles of light intensity and optical depth diminish  
19 during the prolific growth of phytoplankton in surface waters; average daily light exposure for cells will  
20 also diminish during water column structure transitions as observed beyond  $T_2$  where MLD exceeded  
21 the 1% sPAR depth. Under these circumstances, light limitation would be expressed as a preferential use  
22 of  $\text{NH}_4^+$  over  $\text{NO}_3^-$  due to the differential energetic demands (Clark et al., 2002; Flynn et al., 2002). This  
23 was not observed during  $T_{1-2}$ . However,  $\text{NH}_4^+$  assimilation rate consistently exceeded  $\text{NO}_3^-$  assimilation  
24 beyond  $T_3$  (the point at which MLD exceeded the 1% sPAR depth), potentially supporting this  
25 mechanism to describe a characteristic feature of nitrogen assimilation by phytoplankton in upwelled  
26 water (Dickson and Wheeler, 1995; Kudela et al., 1997) and contributing to the progressive decrease in  
27 indicators of phytoplankton activity and biomass.

### 28 29 3.3 The regeneration of inorganic nitrogen.

30 Evidence presented here demonstrated that the regeneration of inorganic nitrogen sustained  
31 phytoplankton productivity during  $P_1$  development. Nutrient regeneration is a product of heterotrophic  
32 DOM degradation by microplankton (bacteria, flagellates, ciliates), following its release from  
33 phytoplankton due to grazing (Probyn, 1987; Varela et al., 2003; Bode et al., 2004) or its active release  
34 from phytoplankton during nutrient assimilation (Bronk et al., 1994; Raimbault and Garcia, 2008;  
35 Benavides et al., 2013). Alternative routes of  $\text{NH}_4^+$  regeneration in upwelling systems may be minor (e.g.  
36 the activity of zooplankton; Bode et al., 2004; Bronk and Steinberg, 2008; Fernández-Urruzola et al.,  
37 2014) or difficult to quantify, such as the contribution from the photochemical degradation of DON  
38 (Rain-Franco et al., 2014).

39 During the present study,  $\text{NH}_4^+$  was regenerated at rates within the range  $9.4\text{--}85.0 \text{ nmol}\cdot\text{L}^{-1}\cdot\text{h}^{-1}$  (Fig.  
40 6). We are unaware of previous studies for the Mauritanian system with which to compare this data. For  
41 Cape Ghir (north of the study location), Benavides et al. (2013) reported  $\text{NH}_4^+$  regeneration rates of

1 8 nmol·L<sup>-1</sup>·h<sup>-1</sup>. For the Benguela system Probyn (1987; 1990) reported rates of 0-125 nmol·L<sup>-1</sup>·h<sup>-1</sup> and  
2 Benavides et al. (2014) reported rates of 90-130 nmol·L<sup>-1</sup>·h<sup>-1</sup>. For the less productive Iberian upwelling  
3 system rates of 0.09-2.52 nmol·L<sup>-1</sup>·h<sup>-1</sup> have been reported (Clark et al., 2011). Benavides et al. (2013)  
4 speculated in their study of the Benguela system that high rates of NH<sub>4</sub><sup>+</sup> regeneration were driven by a  
5 high abundance of dinoflagellates and mixotrophic microflagellates. In the present study, the highest  
6 rate of NH<sub>4</sub><sup>+</sup> regeneration was measured at T<sub>0</sub>, coinciding with the highest ambient ammonium  
7 concentration and abundance of phytoplankton, notably flagellates. This offered circumstantial  
8 evidence supporting a role for microflagellates in NH<sub>4</sub><sup>+</sup> regeneration (Benavides et al., 2013). Conversely,  
9 bacterial abundance derived from analytical flow cytometry (data not shown) did not offer any clear or  
10 statistically significant link with measured rates of NH<sub>4</sub><sup>+</sup> regeneration suggesting that this route may  
11 have been of minor importance. Considering all data, an NH<sub>4</sub><sup>+</sup> pool turnover of 1.2±0.7 d<sup>-1</sup> due to  
12 regeneration and a ratio of 1.7±1.1 for NH<sub>4</sub><sup>+</sup> regeneration to assimilation rate demonstrated the rapidity  
13 of NH<sub>4</sub><sup>+</sup> recycling that was sufficient to meet phytoplankton requirements, as also reported for other  
14 upwelling systems (Benavides et al., 2013; 2014; Raimbault and Garcia, 2008; Clark et al., 2011;  
15 Fernández and Farías, 2012).

16 A sink for regenerated NH<sub>4</sub><sup>+</sup> is the nitrification process. The sequential oxidation of NH<sub>4</sub><sup>+</sup> to NO<sub>2</sub><sup>-</sup> and  
17 NO<sub>3</sub><sup>-</sup> is known not to be restricted to aphotic depths (Raimbault and Garcia, 2008; Clark et al., 2008;  
18 2014) and has been reported in other upwelling systems (Clark et al., 2011; Fernández and Farías, 2012;  
19 Benavides et al., 2014). In their study of the Chilean Upwelling system, Fernández and Farías (2012)  
20 demonstrated that oxygen concentrations have an important influence over nitrogen cycle processes,  
21 influencing the vertical distribution of nitrifying microorganisms. In oxic photic zone conditions  
22 comparable to P<sub>1</sub>, these authors suggested that Crenarchaeota rather than bacteria dominate nitrifying  
23 activity.

24 During the present study, 20±10% of regenerated NH<sub>4</sub><sup>+</sup> entered the nitrification pathway. Rates of  
25 NH<sub>4</sub><sup>+</sup> and NO<sub>2</sub><sup>-</sup> oxidation were 0.30-8.75 nmol·L<sup>-1</sup>·h<sup>-1</sup> and 25.55-81.11 nmol·L<sup>-1</sup>·h<sup>-1</sup> respectively, resulting  
26 in an average turnover of 0.3±0.2 d<sup>-1</sup> and 0.2±0.1 d<sup>-1</sup> for NO<sub>2</sub><sup>-</sup> and NO<sub>3</sub><sup>-</sup> respectively. We are unaware of  
27 previous nitrification rate measurements for the Mauritanian system and as a general observation such  
28 measurements are rare for upwelling systems. For the Benguela system, NO<sub>3</sub><sup>-</sup> regeneration rates of 0.6-  
29 15.5 nmol·L<sup>-1</sup>·h<sup>-1</sup> have been reported (Füssel et al., 2011; Benavides et al., 2014) although in Cape Ghir  
30 nitrification was not detected (Benavides et al., 2013). In the Iberian system, Clark et al. (2011) reported  
31 rates of 0.06-3.74 nmol·L<sup>-1</sup>·h<sup>-1</sup> and 0.04-24.76 nmol·L<sup>-1</sup>·h<sup>-1</sup> for NH<sub>4</sub><sup>+</sup> and NO<sub>2</sub><sup>-</sup> oxidation respectively.

32 The average coupling ratio (NH<sub>4</sub><sup>+</sup>:NO<sub>2</sub><sup>-</sup> oxidation rate) was 0.11±0.07, indicating that these processes  
33 were substantively uncoupled; NO<sub>2</sub><sup>-</sup> oxidation rate exceeded NH<sub>4</sub><sup>+</sup> oxidation rate by several fold as  
34 previously reported (Lipschultz et al., 1990; Beman et al., 2010, 2013; Clark et al., 2011, 2014; Füssel et  
35 al., 2011; Fernández and Farías, 2012; Ganesh et al., 2015). The extent of decoupling would imply that  
36 NO<sub>2</sub><sup>-</sup> oxidation was unsustainable, as NO<sub>2</sub><sup>-</sup> would be removed within 1 day at the prevailing NO<sub>2</sub><sup>-</sup>  
37 oxidation rates. However, a NO<sub>2</sub><sup>-</sup> concentration of approximately 0.3µmol·L<sup>-1</sup> persisted in the photic  
38 zone for the duration of the study indicating an approximate balance between NO<sub>2</sub><sup>-</sup> production and  
39 consumption processes. Füssel et al. (2011) suggested that in suboxic environments associated with the  
40 Namibian oxygen minimum zone, NO<sub>2</sub><sup>-</sup> produced via NO<sub>3</sub><sup>-</sup> reduction (the first stage of denitrification)  
41 could, in combination with NH<sub>4</sub><sup>+</sup> oxidation, support the observed rates of NO<sub>2</sub><sup>-</sup> oxidation. Such a

1 mechanism would be unlikely for the present study as  $P_1$  oxygen concentrations exceeded  $200 \mu\text{mol}\cdot\text{L}^{-1}$   
2 (results not shown), effectively excluding denitrification which is associated with extremely low oxygen  
3 or anoxic conditions (Naqvi et al., 2006). We speculate that these observations could be reconciled by a  
4 mechanism in which particle bound nitrifying organisms existed in close physical and chemical  
5 association. Diverse sources of evidence support this association (Ward, 2008; Ganesh et al., 2015). Via  
6 this mechanism the microbially mediated degradation of particulate organic matter within the  
7 microenvironment of a recently formed biological particle (Stocker, 2012) would regenerate  $\text{NH}_4^+$   
8 directly supporting  $\text{NH}_4^+$  oxidation; resultant  $\text{NO}_2^-$  would support  $\text{NO}_2^-$  oxidation and regenerated  $\text{NO}_3^-$   
9 would be released from particles. In contrast, neither  $\text{NH}_4^+$  nor  $\text{NO}_2^-$  would be released from particles to  
10 an extent that reflected the stoichiometric rate relationships within, or closely associated with the  
11 particle (potentially contributing to the persistent budgetary ' $\text{NH}_4^+$  deficit' previously identified in the  
12 Iberian upwelling study of Clark et al., 2011). If such a mechanism were to operate, specific tracer  
13 methods would underestimate nitrogen regeneration rates (specifically  $\text{NH}_4^+$  regeneration and oxidation  
14 rates) in ecosystems characteristically enriched in newly formed marine particles. If this were the case,  
15 the extent of decoupling would imply that the substantial majority of nitrification within  $P_1$  was  
16 associated with particles. It is unlikely that the micro-environment of marine particles reflects that of  
17 bulk water (Stocker, 2012), offering a rationale for our inability to establish robust relationships  
18 between environmental factors and nitrification rates beyond light inhibition, which has limited model  
19 development (Bouskill et al., 2011; Füssel et al., 2011; Smith et al., 2014a). Additionally, should such a  
20 mechanism operate, particle bound nitrifying organisms would be alleviated to an extent from direct  
21 competition with phytoplankton for  $\text{NH}_4^+$  (Smith et al., 2014b).

22

### 23 3.4 F-ratio formulations.

24 The present study demonstrated that nitrification was measurable from the inception of  $P_1$  implying  
25 that the fraction of regenerated  $\text{NO}_3^-$  progressively increased within days of upwelled water reaching  
26 the photic zone. F-ratio formulations for  $P_1$  are presented in Fig. 7 using simultaneously measured rates  
27 of nitrogen assimilation and regeneration. Using the original formulation, the highest f-ratio values were  
28 derived during the first 3 days of Lagrangian study ( $f=0.44-0.63$ ), generally decreasing as  $P_1$  advected  
29 offshore ( $f=0.32-0.38$ ). A study of this region by Minas et al. (1982) provided an f-ratio value of 0.9 but  
30 did not consider the role of  $\text{NH}_4^+$  regeneration. A revised value of 0.64 was provided by Minas et al.  
31 (1986), comparable to that measured during the earliest stages of this study. Correcting f-ratio values  
32 for isotope dilution ( $f_c$  ratio) made only minor differences. However, accounting for the fraction of  
33 regenerated  $\text{NO}_3^-$  (in addition to isotope dilution;  $f_{\text{regen}}$  ratio) lead to a cumulative decrease in values  
34 relative to the original formulation. Results implied that within approximately 6 days, the fraction of  
35 regenerated  $\text{NO}_3^-$  was greater than 50% and that the transition from 'new' to a 'regenerated'  $\text{NO}_3^-$  pool  
36 occurred rapidly (i.e. the order of days, not weeks). Given the evidence for nitrification in other  
37 upwelling systems (Ward, 2005; Fernández et al., 2009; Clark et al., 2011, Benavides et al., 2014), it is  
38 likely that  $\text{NO}_3^-$  based exportable production from such systems has been over-estimated historically.

39

### 40 3.5. Calculating the carbon export of $P_1$ .

1 Carbon export supported by new production was estimated using the approach of Eppley and  
2 Peterson (1979) as the product of f-ratio and primary production. We compared the original formulation  
3 (f-ratio) to alternative formulations;  $f_c$  ratios (corrected for isotope dilution) and  $f_{\text{regen}}$  ratio (corrected  
4 for isotope dilution and regenerated  $\text{NO}_3^-$ ).

5 Rees et al. (2011) estimated that the time taken for  $P_1$  to mature from newly-upwelled to open ocean  
6 conditions was approximately 14 days, which we confirmed by extrapolation of integrated primary  
7 production rates along an exponential gradient ( $\text{PP} = 801.72 e^{-0.253\text{Time}}$ ,  $r^2 = 0.93$ ). Rates decreased from  
8  $0.69 \text{ molC}\cdot\text{m}^{-2}\cdot\text{d}^{-1}$  ( $T_{-1}$ ) to approximately  $0.02 \text{ molC}\cdot\text{m}^{-2}\cdot\text{d}^{-1}$  on day 14, comparable to rates reported for  
9 the oligotrophic North East Atlantic (Tilstone et al., 2009). The mean area of  $P_1$  was estimated from  
10 surface sea temperature images at  $1.29 \times 10^4 \text{ km}^2$  while upwelling activity characteristics were also  
11 considered. For the purpose of this estimation we assumed that the persistence of upwelling north of  
12  $20^\circ\text{N}$  enabled extrapolation of primary production measured during  $P_1$  over 12 months. By integrating  
13 primary production over the 14 day period between maximum upwelling and open-ocean conditions  
14 and extrapolating to the mean filament area we estimated annual primary production of 12.38 TgC. The  
15 fraction of annual productivity available for export derived using the f-ratio was 6.19 TgC (50%); using  
16 the  $f_c$  ratio exportable production was 6.01 TgC (49%); using the  $f_{\text{regen}}$  ratio exportable production was  
17 4.73 TgC (38%). Comparisons with previous estimations are complicated by differences in filament  
18 location, geographical area, activity, and integration depth, ranging from  $1.12\text{-}2.62 \text{ TgC}\cdot\text{y}^{-1}$  (Helmke et  
19 al., 2005) to  $3.1 \text{ TgC}\cdot\text{y}^{-1}$  (Álvarez-Salgado et al., 2007), which are of similar order to our  $f_{\text{regen}}$  ratio  
20 estimates. Within the constraints of our assumptions, results suggest that both isotope dilution and the  
21 fraction of previously regenerated  $\text{NO}_3^-$  can be important sources of error for nitrogen based  
22 estimations of C-export.

#### 24 4. Conclusions

25 For open ocean systems, the limitation to the new production paradigm that  $\text{NO}_3^-$  is not necessarily  
26 'new' is now well established; to this we add that even within upwelling regions where genuinely new  
27  $\text{NO}_3^-$  is supplied to the photic zone, the fraction of regenerated  $\text{NO}_3^-$  increases rapidly. Since the  
28 instantaneous ratio of new to regenerated  $\text{NO}_3^-$  cannot readily be derived this adds uncertainty to f-  
29 ratio values. Upwelling zones are unquestionably highly productive. However, our data indicate that  
30 nitrification in these waters is significant. It impacts upon f-ratio derived estimations of new production  
31 and carbon export by diluting  $^{15}\text{NO}_3^-$  tracer and facilitating a transition in  $\text{NO}_3^-$  pool provenance from a  
32 source of 'new' towards a source of 'regenerated' nitrogen.

#### 34 Acknowledgements

35 We thank Carol Robinson (chief scientist), Ricardo Torres and Phil Nightingale for cruise leadership and  
36  $\text{SF}_6$  mapping, and the officers and crew of the RRS Discovery cruise D338. We thank NEODAAS for  
37 providing satellite data to SOLAS-ICON. We thank Lisa Al-Moosawi for isotope ratio mass-spectrometry  
38 analysis and two anonymous reviewers for constructive comments during the review process. This study  
39 was supported by NERC grant NE/C517176/1 (UK-SOLAS) and by Theme 2 of NERC Oceans 2025.

#### 41 References

- 1 Álvarez-Salgado, X.A., Beloso, S., Joint, I., Nogueira, E., Chou, L., Perez, F.F., Groom, S., Cabanas, J.M.,  
2 Rees, A.P. and Elskens, M.: New production of the NW Iberian shelf during the upwelling season over  
3 the period 1982–1999, *Deep-Sea Res. Part I*, 49, 1725–1739, doi:10.1016/S0967-0637(02)00094-8,  
4 2002.
- 5
- 6 Álvarez-Salgado, X. A., Arístegui, J., Barton, E.D. and Hansell, D. A.: Contribution of upwelling filaments  
7 to offshore carbon export in the subtropical Northeast Atlantic Ocean. *Limnol. Oceanogr.* 52, 1287-1292,  
8 doi:10.4319/lo.2007.52.3.12872007, 2007.
- 9
- 10 Arístegui, J., Álvarez-Salgado, X.A., Barton, E.D., Figueiras, F.G., Hernández-León, S., Roy, C. and Santos,  
11 A.M.P.: Oceanography and fisheries of the Canary Current Iberian region of the Eastern North Atlantic,  
12 p. 877–931. In A. Robinson and K. H. Bronk [eds.], *The global coastal ocean: Interdisciplinary regional  
13 studies and syntheses*. Harvard Univ. Press, 2006.
- 14
- 15 Arístegui, J., Barton, E.D., Álvarez-Salgado, X. A., Santos, M. P., Figueiras, F. G., Kifani, S., Hernández-  
16 León, S., Mason, E., Machú, E. and Demarcq, H.: Sub-regional ecosystem variability in the Canary Current  
17 upwelling, *Prog. Oceanogr.* 83, 33-43, 2009. doi:10.1016/j.pocean.2009.07.031, 2009.
- 18
- 19 Baker, A.R., Kelly, S.D., Biswa, K.F., Witt, M. and Jickells, T.D.: Atmospheric deposition of nutrients to the  
20 Atlantic Ocean, *Geophys. Res. Lett.* 30, 2296, doi:10.1029/2003GL018518, 2003
- 21
- 22 Beman, J.M., Sachdeva, R. and Fuhrman, J.A.: Population ecology of nitrifying Archaea and bacteria in  
23 the Southern California Bight. *Environmental Microbiology.* 12, 1282-1292, doi:10.1111/j.1462-  
24 2920.2010.02172.x, 2010.
- 25
- 26 Beman, J.M., Shih, J.L. and Popp, B.N.: Nitrite oxidation in the upper water column and oxygen minimum  
27 zone of the eastern tropical North Pacific Ocean, *Int. Soc. Micro. Ecol.* 7, 2192-2205,  
28 doi:10.1038/ismej.2013.96, 2013.
- 29
- 30 Benavides M., Arístegui, J., Agawin, N.S.R., Álvarez-Salgado, X.A., Álvarez, M., and Troupin, C.: Low  
31 contribution of N<sub>2</sub> fixation to new production and excess nitrogen in the subtropical northeast Atlantic  
32 margin, *Deep-Sea Res., I*, 81, 36-48, doi:10.1016/j.dsr.2013.07.004, 2013.
- 33
- 34 Benavides M., Santana-Falcón Y., Wasmund, N. and Arístegui, J.: Microbial uptake and regeneration of  
35 inorganic nitrogen off the coastal Namibian upwelling system. *J. Mar. Sys.* 140, 123-129,  
36 doi:10.1016/j.jmarsys.2014.05.002, 2014.
- 37
- 38 Blackburn, T.H.: Method for measuring rates of NH<sub>4</sub><sup>+</sup> turnover in anoxic marine sediments, using <sup>15</sup>N-  
39 NH<sub>4</sub><sup>+</sup> dilution technique, *Appl. Environ. Microbiol.* 37, 760–765, 1979.
- 40
- 41 Bode, A., Barquero, S., Gonzalez, N., Alvarez-Ossorio, M. T., and Varela, M.: Contribution



1 of heterotrophic plankton to nitrogen regeneration in the upwelling ecosystem of A Coruña (NW  
2 Spain), *J. Plankton Res.* 26, 11–28, doi:10.1093/plankt/fbh003, 2004.

3

4 Bouskill, N.J., Eveillard, D., Chien, D., Jayakumar, A. and Ward, B.B: Environmental factors determining  
5 ammonia-oxidizing organism distribution and diversity in marine environments, *Env. Microbiol*, 14, 714-  
6 729, doi:10.1111/j.1462-2920.2011.02623.x, 2011.

7

8 Bronk, D.A. and Glibert, P.M.: Contrasting patterns of dissolved organic nitrogen release by two size  
9 fractions of estuarine plankton during a period of rapid  $\text{NH}_4^+$  consumption and  $\text{NO}_2^-$  production, *Mar.*  
10 *Ecol. Prog. Ser.* 96, 291-299, 1993.

11

12 Bronk, D.A. and Ward, B.B.: Gross and net nitrogen uptake and DON release in the euphotic zone of  
13 Monterey Bay, California, *Limnol. Oceanogr.* 44, 573-585, 1999.

14

15 Bronk, D.A. and Steinberg, D.K.: Nitrogen regeneration. In: *Nitrogen in the Marine Environment*, Capone,  
16 D., Bronk, D.A., Mulholland, M.R., Carpenter, E.J. (eds). Elsevier Press, pp 385-467, 2008.

17

18 Bronk, D.A., Glibert, P.M. and Ward, B.B.: Nitrogen uptake, dissolved organic nitrogen release, and new  
19 production, *Science*, 265:1843, doi:10.1126/science.265.5180.1843, 1994.

20

21 Brzezinski, M. A.: The Si-C-N ratio of marine diatoms—Interspecific variability and the effect  
22 of some environmental variables. *J. Phycol.* 21, 347–357, doi:10.1111/j.0022-3646.1985.00347.x, 1985.

23

24 Caperon, J., Schell, D., Hirota, J. and Laws, E: Ammonium excretion rates in Kaneohe Bay, Hawaii,  
25 measured by a  $^{15}\text{N}$  isotope dilution technique, *Mar. Biol.* 54, 33–40, doi:10.1007/BF00387049, 1979.

26

27 Chavez, F. and Messié, M.: A comparison of Eastern Boundary Upwelling Ecosystems, *Prog. Oceanogr.* 83,  
28 80-96, doi:10.1016/j.pcean.2009.07.32, 2009.

29

30 Clark, D.R., Flynn, K.J. and Owens, N.J.P.: The large capacity for dark nitrate-assimilation in diatoms may  
31 overcome nitrate limitation of growth, *New Phytologist*, doi:10.1046/j.1469-8137.2002.00435.x, 155:  
32 101–108, 2002.

33

34 Clark, D.R., Fileman, T.W. and Joint, I.: Determination of ammonium regeneration rates in the  
35 oligotrophic ocean by gas chromatography/mass spectrometry, *Mar. Chem.* 98, 121-130,  
36 doi:10.1016/j.marchem.2005.08.006, 2006.

37

38 Clark, D.R., Rees, A.P. and Joint, I.: A method for the determination of nitrification rates in oligotrophic  
39 marine seawater by gas chromatography/mass spectrometry, *Mar. Chem.* 103: 84-96,  
40 doi:10.1016/j.marchem.2006.06.005, 2007.

41

- 1 Clark, D.R., Rees, A.P. and Joint, I.: Ammonium regeneration and nitrification rates in the oligotrophic  
2 Atlantic Ocean: Implications for new production estimates, *Limnol. Oceanogr.* 53: 52–62,  
3 doi:10.4319/lo.2008.53.1.0052, 2008.  
4
- 5 Clark, D.R., Miller, P.I., Woodward, E.M.S. and Rees, A.P.: Inorganic nitrogen assimilation and  
6 regeneration in the coastal upwelling region of the Iberian Peninsula, *Limnol. Oceanogr.* 56, 1689–1702,  
7 doi:10.4319/lo.2011.56.5.1689, 2011.  
8
- 9 Clark, D.R., Brown, I.J., Rees, A.P., Somerfield, P.J. and P. I. Miller.: The influence of ocean acidification  
10 on nitrogen regeneration and nitrous oxide production in the northwest European shelf sea,  
11 *Biogeosciences*, 11, 4985–5005, doi:10.5194/bg-11-4985-2014, 2014.  
12
- 13 D’Asaro, E.A.: Lagrangian trajectories on the Oregon shelf during upwelling, *Cont. Shelf Res.*, 24(13–14),  
14 1421–1436, doi:10.1016/j.csr.2004.06.003, 2004.  
15
- 16 Dickson, M.L. and Wheeler, P.A.: Nitrate uptake rates in a coastal upwelling regime – A comparison of  
17 PN-specific, absolute and chl a-specific rates, *Limnol. Oceanogr.* doi:10.4319/lo.1995.40.3.0533, 40, 533-  
18 543, 1995.  
19
- 20 Deutsch, C., Sarmiento, J.L., Sigman, D.M., Gruber, N. and Dunne, J.P.: Spatial coupling of nitrogen inputs  
21 and losses in the ocean, *Nature*, 445, 163–167, doi:10.1038/nature05392, 2007.  
22
- 23 Dugdale, R.C., and Goering, J.J.: Uptake of new and regenerated forms of nitrogen in primary  
24 productivity, *Limnol. Oceanogr.* 12, 196–206, doi:10.4319/lo.1967.12.2.0196, 1967.  
25
- 26 Dugdale, R.C., Wilkerson, F.P. and Morel, A.: Realization of new production in coastal upwelling areas: A  
27 means to compare relative performance, *Limnol. Oceanogr.* 35, 822–829,  
28 doi:10.4319/lo.1990.35.4.0822, 1990.  
29
- 30 Eppley, R.W. and Peterson, B.J.: Particulate organic matter flux and planktonic new production in the  
31 deep ocean, *Nature*, 282, 677–680, doi:10.1038/282677a0, 1979.  
32
- 33 Fernández, C. and Farías, L.: Assimilation and regeneration of inorganic nitrogen in a coastal upwelling  
34 system: ammonium and nitrate utilisation, *Mar. Ecol. Prog. Ser.* 451:1–14, doi:10.3354/meps09683,  
35 2012.  
36
- 37 Fernández, C., Raimbault, P., Garcia, N. and Rimmelin, P.: An estimation of annual new production and  
38 carbon fluxes in the northeast Atlantic Ocean during 2001, *J. Geophys. Res.*, 110, C07S13,  
39 doi:10.1029/2004JC002616, 2005.  
40

1 Fernández, C., Farías, L. and Alcaman, M.E.: Primary production and nitrogen regeneration processes in  
2 surface waters of the Peruvian upwelling system, *Prog. Oceanogr.* 83, 159–168,  
3 doi:10.1016/j.pocean.2009.07.010, 2009.  
4

5 Fernández-Urruzola, I., Osma, N., Packard, T.T., Gómez, M. and Postel, L.: Distribution of zooplankton  
6 biomass and potential metabolic activities across the northern Benguela upwelling system, *Journal of*  
7 *Marine Systems*. 140: 138-149, doi:10.1016/j.jmarsys.2014.05.009, 2014.  
8

9 Flohr, A., van der Plas, A.K., Emeis, K.-C., Mohrholz, V. and Rixen, T.: Spatio-temporal patterns of C:N:P  
10 ratios in the northern Benguela upwelling system, *Biogeosciences*, 11, 885-897, doi:10.5194/bg-11-885-  
11 2014, 2014.  
12

13 Flynn, K.J., Clark, D.R. and Owens, N.J.P.: Modelling suggests that optimization of dark  
14 nitrogen-assimilation need not be a critical selective feature in phytoplankton, doi:10.1046/j.1469-  
15 8137.2002.00436.x, *New Phytologist* 155: 109–119, 2002.  
16

17 Füssel, J., Lam, P., Lavik, G., Jensen, M.M., Holtappels, M., Günter, M. and Kuypers, M.M.M.: Nitrite  
18 oxidation in the Namibian oxygen minimum zone, *ISME Journal* 1-10, doi:10.1038/ismej.2011.178, 2011.  
19

20 Ganesh, S. Bristow, L.A., Larsen, M., Sarode, N., Thamdrup, B. and Stewart, F.J.: Size-fraction partitioning  
21 of community gene transcription and nitrogen metabolism in a marine oxygen minimum zone, *ISME*, 9,  
22 2682–2696, doi:10.1038/ismej.2015.44, 2015.  
23

24 Gilpin, L.C., Davidson, K. and Roberts, E.: The influence of changes in nitrogen: silicon ratios on  
25 diatom growth dynamics, *J. Sea Res.* 51, 21-35, doi:10.1016/j.seares.2003.05.005, 2004.  
26

27 Glibert, P.M., Lipshultz, F., McCarthy, J.J. and Altabet, M.A.: Isotope dilution models of  
28 uptake and remineralization of ammonium by marine plankton, *Limnol. Oceanogr.* 27, 639–650,  
29 doi:10.4319/lo.1982.27.4.0639, 1982.  
30

31 Gregor, L. and Monteiro, P.M.S.: Seasonal cycle of N:P:TA stoichiometry as a modulator of CO<sub>2</sub> buffering  
32 in eastern boundary upwelling systems, *Geophys. Res. Lett.* 40, 5429-5434, doi:10.1002/2013GL058036,  
33 2013  
34

35 Helmke, P., Romero, O. and Fischer, G.: Northwest African upwelling and its effect on offshore organic  
36 carbon export to the deep sea, *Global Biogeochem. Cyc.* 19, GB4015, doi:10.1029/2004GB002265,  
37 2005.  
38

39 Intergovernmental Oceanographic Commission, Paris (France), Protocols for the Joint Global Flux Study  
40 (JGOFS) core measurements, *Manuals Guides* 29, 1994.  
41

1 Jickells, T. and Moore, C.M.: The importance of atmospheric deposition for ocean productivity, *Annu.*  
2 *Rev. Ecol. Evol. Syst.*, 46:481-501, doi:10.1146/annurev-ecolsys-112414-054118, 2015.

3

4 Joint, I., Rees, A.P. and Woodward, E.M.S.: Primary production and nutrient assimilation in the Iberian  
5 upwelling in August 1998, *Prog. Oceanogr.* 51, 303–320, doi:10.1016/S0079-6611(01)00072-6, 2001a.

6

7 Joint, I., Inall, M., Torres, R., Figueiras, F.G., Álvarez-Salgado, X.A., Rees, A.P. and Woodward, E.M.S.: Two  
8 Lagrangian experiments in the Iberian Upwelling System: Tracking an upwelling event and an offshore  
9 filament, *Prog. Oceanogr.*, 51(2–4), 221–248, doi:10.1016/S0079-6611(01)00068-4, 2001b.

10

11 Kanda, J., Laws, E.A., Saino, S.T. and Hattori, A.: An evaluation of isotope dilution effect from  
12 conventional data sets of <sup>15</sup>N uptake experiments, *J. Plankton Res.* 19, 79–90,  
13 doi:10.1093/plankt/9.1.79, 1987.

14

15 Kudela, R.M., Cochlan, W.P. and Dugdale, R.C.: Carbon and nitrogen uptake response to light by  
16 phytoplankton during an upwelling event, *J. Plankton Res.* 19, 609-630, doi:10.1093/plankt/19.5.609,  
17 1997.

18

19 Loucaides, S., Tyrrell, T., Achterberg, E.P., Torres, R., Nightingale, P.D., Kitidis, V., Serret, P., Woodward,  
20 M. and Robinson, C.: Biological and physical forcing of carbonate chemistry in an upwelling filament off  
21 northwest Africa: Results from a Lagrangian study, *Global Biogeochemical Cycles.* 26:GB3008,  
22 doi:10.1029/2011GB004216, 2012.

23

24 Lipshultz, F., Wofsy, S.C., Ward, B.B., Codispoti, L.A., Freidrich, G. and Elkins, J.W.: Bacterial  
25 transformations of inorganic nitrogen in the oxygen deficient waters of the Eastern Tropical South  
26 Pacific Ocean, *Deep Sea Res.* 37, 1513-1541, 1990.

27

28 Martin, A.P. and Pondaven, P.: New production and nitrification in the western subtropical North  
29 Atlantic: A modelling study, *Global Biogeochem. Cyc.* 20, GB4014, doi:10.1029/2005GB002608, 2006.

30

31 Meunier, T., Barton, E.D., Barreiro, B. and Torres, R.: Upwelling filaments off Cap Blanc: Interaction of  
32 the NW African upwelling current and the Cape Verde frontal zone eddy field? *J. Geophys. Res.* 117,  
33 C08031, doi:1029/2012JC007905, 2012.

34

35 Miller, P., Groom, S., McManus, A., Selley, J. and Mironnet, N.: Panorama: A semi-automated AVHRR  
36 and CZCS system for observation of coastal and ocean processes, *RSS97: Observations and Interactions,*  
37 *Proceedings of the Remote Sensing Society,* 539-544, 1997.

38

39 Minas, T., Packard, T., Minas, M., Coste, B.: An analysis of the production-regeneration system in the  
40 coastal upwelling area off N.W. Africa based on oxygen, nitrate and ammonium distribution. *J. Mar. Res.*  
41 40, 615-641, 1982.

1  
2 Minas, H.J., Minas, M., Packard, T.T.: Productivity in upwelling areas deduced from hydrographic and  
3 chemical fields, *Limnol. Oceanogr.* 31(6), 1182-1206, 1986.  
4  
5 Mitra, A., Flynn, K.J., Burkholder, J.M., Berge, T., Calbet, A., Raven, J.A., Granéli, E., Glibert, P.M., Hansen,  
6 P.J., Stoecker, D.K., Thingstad, F., Tillmann, U., Våge, S., Wilken, S. and Zubkov, M.V.: The role of  
7 mixotrophic protists in the biological carbon pump, *Biogeosciences*, 11, 995-1005, doi:10.5194/bg-11-  
8 995-2014, 2014.  
9  
10 Mittelstaedt, E.: The ocean boundary along the northwest African coast: Circulation and oceanographic  
11 properties at the sea surface, *Prog. Oceanogr.* 26, 307-355, doi:10.1016/0079-6611(91)90011-A, 1991.  
12  
13 Moore, C.M., Mills, M.M., Achterberg, E.P., Geider, R.J., LaRoche, J., Lucas, M.I., McDonagh, E.L., Pan, X.,  
14 Poulton, A.J., Rijkenberg, M.J.A., Suggett, D., Ussher, S.J. and Woodward, E.M.S.: Large-scale distribution  
15 of Atlantic nitrogen fixation controlled by iron availability, *Nature Geoscience*, 2, 867-871,  
16 doi:10.1038/ngeo667, 2009.  
17  
18 Moore, C.M., Mills, M.M., Arrigo, K.R., Berman-Frank, I., Bopp, L., Boyd, P.W., Galbraith, E.D., Geider,  
19 R.J., Guieu, C., Jaccard, S.L., Jickells, T.D., La Roche, J., Lenton, T.M., Mahowald, N.M., Marañón, E.,  
20 Marinov, I., Moore, J.K., Nakatsuka, T., Oschlies, A., Saito, M.A., Thingstad, T.F., Tsuda, A. and Ulloa, O.:  
21 Processes and patterns of oceanic nutrient limitation. *Nature Geoscience*, 6, 701-710,  
22 doi:10.1038/ngeo1765, 2013.  
23  
24 Moschonas, G., Gowen, R.J., Stewart, B.M. and Davidson, K.: Nitrogen dynamics in the Irish Sea and  
25 adjacent shelf waters: An exploration of dissolved organic nitrogen, *Estuarine, Coastal and Shelf Science*,  
26 164, 276-287, doi:10.1016/j.ecss.2015.07.030, 2015.  
27  
28 Naqvi, S.W.A., Naik, H., Pratihary, A., D'Souza, W., Narvekar, P.V., Jayakumar, D.A., Devol, A.H.,  
29 Yoshinari, T. and T. Saino.: Coastal versus open-ocean denitrification in the Arabian Sea, *Biogeosciences*,  
30 3, 621-633, doi:10.5194/bg-3-621-2006, 2006.  
31  
32 Nightingale, P.D., Malin, G., Law, C.S., Watson, A.J., Liss, P.S., Liddicoat, M.I., Boutin, J. and Upstill-  
33 Goddard, R.C.: In situ evaluation of air-sea gas exchange parameterizations using novel conservative and  
34 volatile tracers, *Global Biogeochem. Cyc.* 14, 373-387, doi:10.1029/1999GB900091, 2000.  
35  
36 Nowald, N., Iversen, M.H., Fischer, G., Ratmeyer, V., Wefer, G.: Time series of *in-situ* particle properties  
37 and sediment trap fluxes in the coastal upwelling filament off Cape Blanc, Mauritania, *Prog. Oceanogr.*  
38 137, 1-11, doi:10.1016/j.pocean.2014.12.015.  
39  
40 Olson, R.J.: Differential photoinhibition of marine nitrifying bacteria: a possibly mechanisms for the  
41 formation of the primary nitrite maximum, *J. Mar. Res.* 39, 227-238, 1981.

1  
2 Pauly, D. and Christensen, V.: Primary production required to sustain global fisheries, *Nature*, 374(6519),  
3 255–257, doi:10.1038/374255a0, 1995.  
4  
5 Postel, L., Mohrholz, V. and Packard, T.T.: Upwelling and successive ecosystem response in the Northern  
6 Benguela Region - an in situ experiment, *Journal of Marine Systems* 140, 73–81,  
7 doi:10.1016/j.jmarsys.2014.07.014, 2014.  
8  
9 Powell, C.F., Baker, A.R., Jickells, T.D., Bange, H.W., Chance, R.J., and Yodle, C.: Estimation of the  
10 Atmospheric Flux of Nutrients and Trace Metals to the Eastern Tropical North Atlantic Ocean, *J. Atm.*  
11 *Sci.*, 72: 4029-4045, doi: 10.1175/JAS-D-15-0011.1, 2015.  
12  
13 Probyn, T.A.: Ammonium regeneration by microplankton in an upwelling environment, *Mar.*  
14 *Ecol. Prog. Ser.* 37, 53–64, 1987.  
15  
16 Probyn, T.A.: Size-fractionated measurements of nitrogen uptake in aged upwelled waters: Implications  
17 for pelagic food webs. *Limnol. Oceanogr.* 35, 202–210, doi:10.4319/lo.1990.35.1.0202, 1990.  
18  
19 Raimbault, P. and Garcia, N.: Evidence for efficient regenerated production and dinitrogen fixation in  
20 nitrogen-deficient waters of the South Pacific Ocean: impact on new and export production estimates,  
21 *Biogeosciences*, 5, 323-338, doi:10.5194/bg-5-323-2008, 2008.  
22  
23 Rain-Franco, A., Muñoz, C. and Fernández, C.: Ammonium production off central Chile (36°S) by  
24 photodegradation of phytoplankton derived and marine dissolved organic matter, *PLoSOne*, 9, e100224,  
25 doi:10.1371/journal.pone.0100224, 2014.  
26  
27 Rees, A.P., Brown, I.J., Clark, D.R. and Torres, R.: The Lagrangian progression of nitrous oxide within  
28 filaments formed in the Mauritanian upwelling, *Geophys. Res. Lett.* 38, L21606,  
29 doi:10.1029/2011GL049322, 2011.  
30  
31 Santoro, A.E., Casciotti, K.L. and Francis, C.A.: Activity, abundance and diversity of nitrifying archaea and  
32 bacteria in the central California Current, *Environ. Microbiol.* 12, 1989–2006, doi:10.1111/j.1462-  
33 2920.2010.02205.x, 2010.  
34  
35 Shannon, L.V. and Field, J.G.: Are fish stocks food limited in the southern Benguela pelagic ecosystem?  
36 *Mar. Ecol. Prog. Ser.* 22, 7–19, doi:10.3354/meps022007, 1985.  
37  
38 Smith, J.M., Casciotti, K.L., Chavez, F.P., Francis, C.A.: Differential contribution of archaeal ammonia  
39 oxidizer ecotypes to nitrification in coastal surface waters, *ISME*, 8, 1704-1714,  
40 doi:10.1038/ismej.2014.11, 2014a.  
41

1 Smith, K.M., Chavez, F.P. and Francis, C.A.: Ammonium uptake by phytoplankton regulates nitrification  
2 in the sunlit ocean. *PLoS ONE* 9:e108173, doi:10.1371/journal.pone.0108173, 2014b.  
3

4 Sohm, J., Hilton, J., Noble, A.E., Zehr, J.P., Saito, M. and Webb, E.A.: Nitrogen fixation in the South  
5 Atlantic Gyre and the Benuela Upwelling System, *Geophys. Res. Lett.*, 38, L16608,  
6 doi:10.1029/2011GL048315, 2011  
7

8 Staal, M.S., Lintel Heckert, S., Brummer, G.J.A., Veldhuis, M., Sikkens, C., Persijn, S. and Stal, L.J.:  
9 Nitrogen fixation along north-south transect in the eastern Atlantic ocean, *Limnol. Oceanogr.*, 52, 1305-  
10 1316, doi:10.4319/lo.2007.52.4.1305, 2007.  
11

12 Stocker, R.: Marine microbes see a sea of gradients, *Science*, 338, 628-633, 2012,  
13 doi:10.1126/science.1208929.  
14

15 Sweeney, R.E., Liu, K.K. and Kaplan, I.R.: Oceanic nitrogen isotopes and their uses in determining the  
16 source of sedimentary nitrogen, *N. Z. Depart. Sci. Ind. Res. Bull.* 220, 9–26, 1978.  
17

18 Tilstone, G., Smyth, T., Poulton, A. and Hutson, R.: Measured and remotely sensed estimates of primary  
19 production in the Atlantic Ocean from 1998 to 2005, *Deep-Sea Res (II)*, 56, 918-930,  
20 doi:10.1016/j.dsr2.2008.10.034, 2009.  
21

22 Tomczak, M. and Godfrey, J.S.: *Regional Oceanography: An Introduction* (second ed) Daya, Delhi, India,  
23 p. 390, 2003.  
24

25 Varela, M.M., Barquero, S., Bode, A., Fernández, E., González, N., Teira, E. and Varela, M.:  
26 Microplanktonic regeneration of ammonium and dissolved organic nitrogen in the upwelling area of the  
27 NW of Spain: relationships with dissolved organic carbon production and phytoplankton size-structure,  
28 *J. Plank. Res.*, 25, 719-736, 2003.  
29

30 Varela, M., Bode, A., Fernández, E., Gonzales, N., Kitidis, V., Varela, M., and Woodward, E.M.S.: Nitrogen  
31 uptake and dissolved organic nitrogen release in planktonic communities characterized by  
32 phytoplankton size structure in the central North Atlantic, *Deep Sea Res. I*, 52, 1637–1661,  
33 doi:10.1016/j.dsr.2005.03.007, 2005.  
34

35 Wafar, M., L'Helguen, S., Raikar, V., Maguer, J.F., Corre, P.L.: Nitrogen uptake by size-fractionated  
36 plankton in permanently well-mixed temperate coastal waters, *J. Plank. Res.* 26, 1207-1218,  
37 doi:10.1093/plankt/fbh110, 2004.  
38

39 Ward, B.B.: Temporal variability in nitrification rates and related biogeochemical factors in Monterey  
40 Bay, California, USA, *Mar. Ecol. Prog. Ser.* 292, 97-109, doi:10.3354/meps292097, 2005.  
41

1 Ward, B.: Nitrogen in the Marine Environment, In: Nitrogen in the Marine Environment, Capone, D.,  
2 Bronk, D.A., Mulholland, M.R., Carpenter, E.J. (eds). Elsevier Press, pp 199-261, 2008.  
3  
4 Wasmund, N., Struck, U., Hansen, A., Flohr, A., Nausch, G., Gruttmuller, A., and Voss, M.: Missing  
5 nitrogen fixation in the Benguela region, Deep-Sea Res. I, 106, 30-41, doi:10.1016/j.dsr.2015.10.007,  
6 2015.  
7  
8 Wilkerson, F. P. and Dugdale, R.C.: The use of large shipboard barrels and drifters to study the effects of  
9 coastal upwelling on phytoplankton dynamics, Limnol. Oceanogr., 32(2), 368–382,  
10 doi:10.4319/lo.1987.32.2.0368, 1987.  
11  
12 Wilkerson, F.P. and Dugdale, R.C.: Coastal Upwelling, In: Nitrogen in the Marine Environment, Capone,  
13 D., Bronk, D.A., Mulholland, M.R., Carpenter, E.J. (eds). Elsevier Press, pp 765-801, 2008.  
14  
15 Woodward, E.M.S. and Rees, A.P.: Nutrient distributions in an anticyclonic eddy in the North East  
16 Atlantic Ocean, with reference to nanomolar ammonium concentrations, Deep-Sea Res. 48, 775–794,  
17 doi:10.1016/S0967-0645(00)00097-7, 2001.  
18  
19 Zindler, C., Peeken, I., Marandino, C.A. and Bange, H.W.: Environmental control on the variability of DMS  
20 and DMSP in the Mauritanian upwelling region, Biogeosciences, 9, 1041–1051, doi:10.5194/bg-9-1041-  
21 2012, 2012.



1 **Figure legends**

2 Fig. 1. Panel (a) presents composite sea-surface chlorophyll 'a' (April 20-30<sup>th</sup>, 2009) of the sampling area.  
3 The station locations are identified as white squares. Panel (b) presents the daily lateral SF<sub>6</sub>/<sup>3</sup>He  
4 distribution, defined as 40% of the peak concentration. The red line indicates the track of a central  
5 marker buoy used in combination with SF<sub>6</sub>/<sup>3</sup>He analysis. Panel (c) presents water column temperature  
6 (°C) and includes sampling depths for 55% sPAR (black circles) and 1% sPAR (blue squares). The depth of  
7 the upper mixed layer is indicated (red triangles; Loucaides et al., 2012). Note the reversal of dates in  
8 panel (c) to aid comparisons between figures.

9  
10 Fig. 2. Average concentration of inorganic nutrients within the upper mixed layer; (a) nitrate, (b) nitrite,  
11 (c) ammonium, (d) phosphate, (e) silicate. The phosphate excess (P\*) is presented in panel (f). Error bars  
12 represent one standard deviation for triplicate concentration measurements. Note the reversal of dates  
13 to aid comparisons between figures.

14  
15 Fig. 3. Ratio between ambient concentrations of nitrate and phosphate. The solid regression line is the  
16 Redfield ratio of 16:1. Data from within the surface mixed layer depth (MLD) are presented in panel (a),  
17 the regression of which provides a ratio of 13.9:1 and a phosphate excess of 72±18 nmol-P·L<sup>-1</sup>. Data  
18 from below the MLD, presented in panel (b) were collected to a maximum depth of 1.4 km. The  
19 regression of this data provided a ratio of 17.7:1.

20  
21 Fig 4. Changes in integrated (photic depth) primary production and integrated chlorophyll concentration  
22 in two size fraction (> 2µm and 0.2-2µm). Note the reversal of dates to aid comparisons between  
23 figures.

24  
25 Fig.5. Changes in the abundance of phytoplankton (a), the concentration of particulate organic nitrogen  
26 (PON, b), and the rate of nitrogen assimilation as nitrate and ammonium (c). PON and nitrogen  
27 assimilation were measured within the mixed layer at 55% sPAR. Error bars represent one standard  
28 deviation for triplicate concentration (b) or rate (c) measurements. Note the reversal of dates to aid  
29 comparisons between figures.

30  
31 Fig. 6. Changes in the rate of ammonium regeneration (a), ammonium oxidation (b) and nitrite oxidation  
32 (c) for samples taken within the mixed layer depth at 55% and 1% sPAR. Error bars represent one  
33 standard deviation for triplicate rate measurements. Note the reversal of dates to aid comparisons  
34 between figures.

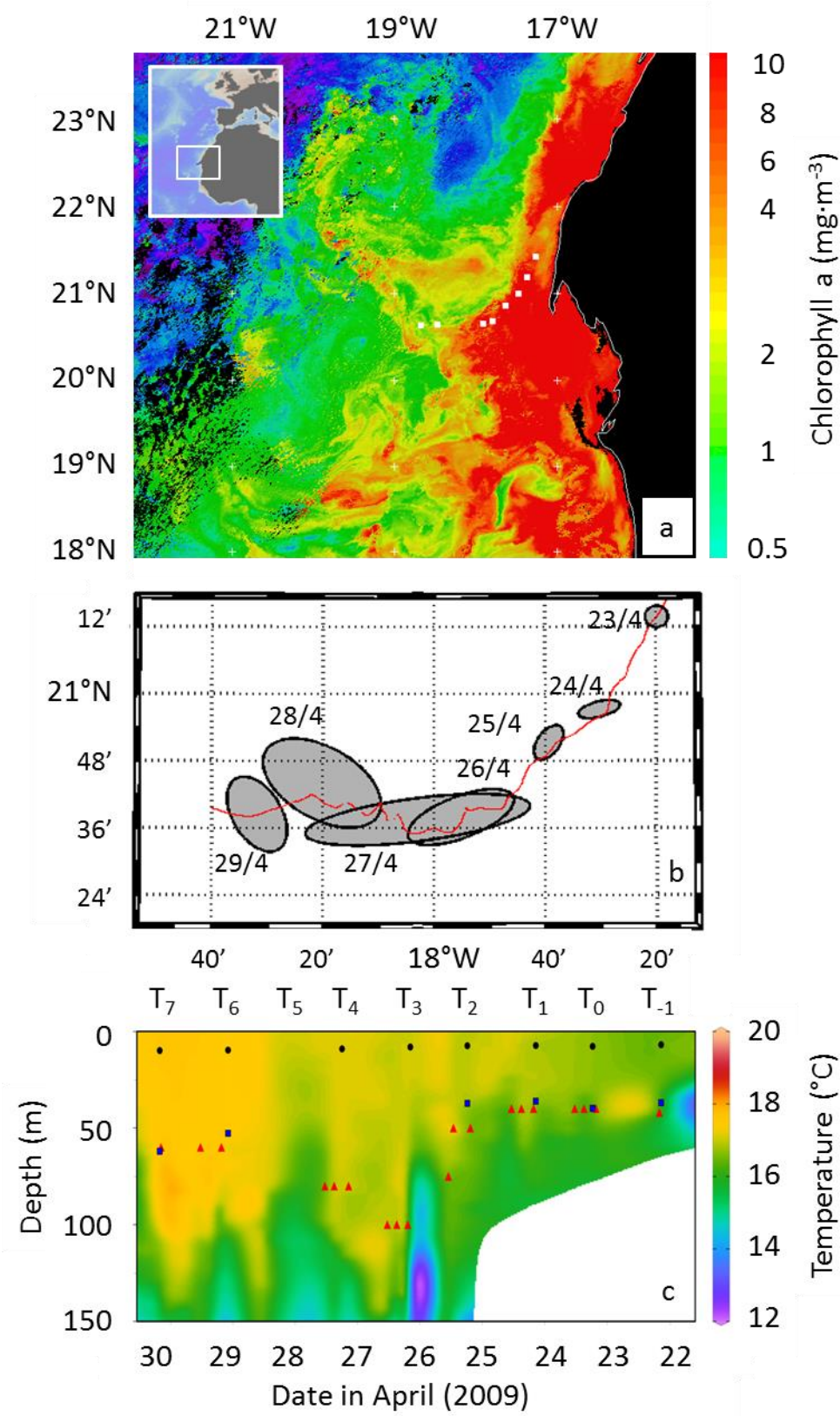
35  
36 Fig. 7. Changes in f-ratio representations (f-ratio; f<sub>c</sub>-ratio corrected for isotope dilution due to nitrogen  
37 regeneration; f<sub>regen</sub>-ratio corrected for isotope dilution and the fraction of the nitrate pool represented  
38 by 'new' rather than 'regenerated' nitrate. The fraction of the nitrate pool represented by 'new' nitrate  
39 is also presented (R<sub>NO3</sub>). Note the reversal of dates to aid comparisons between figures.

40

41

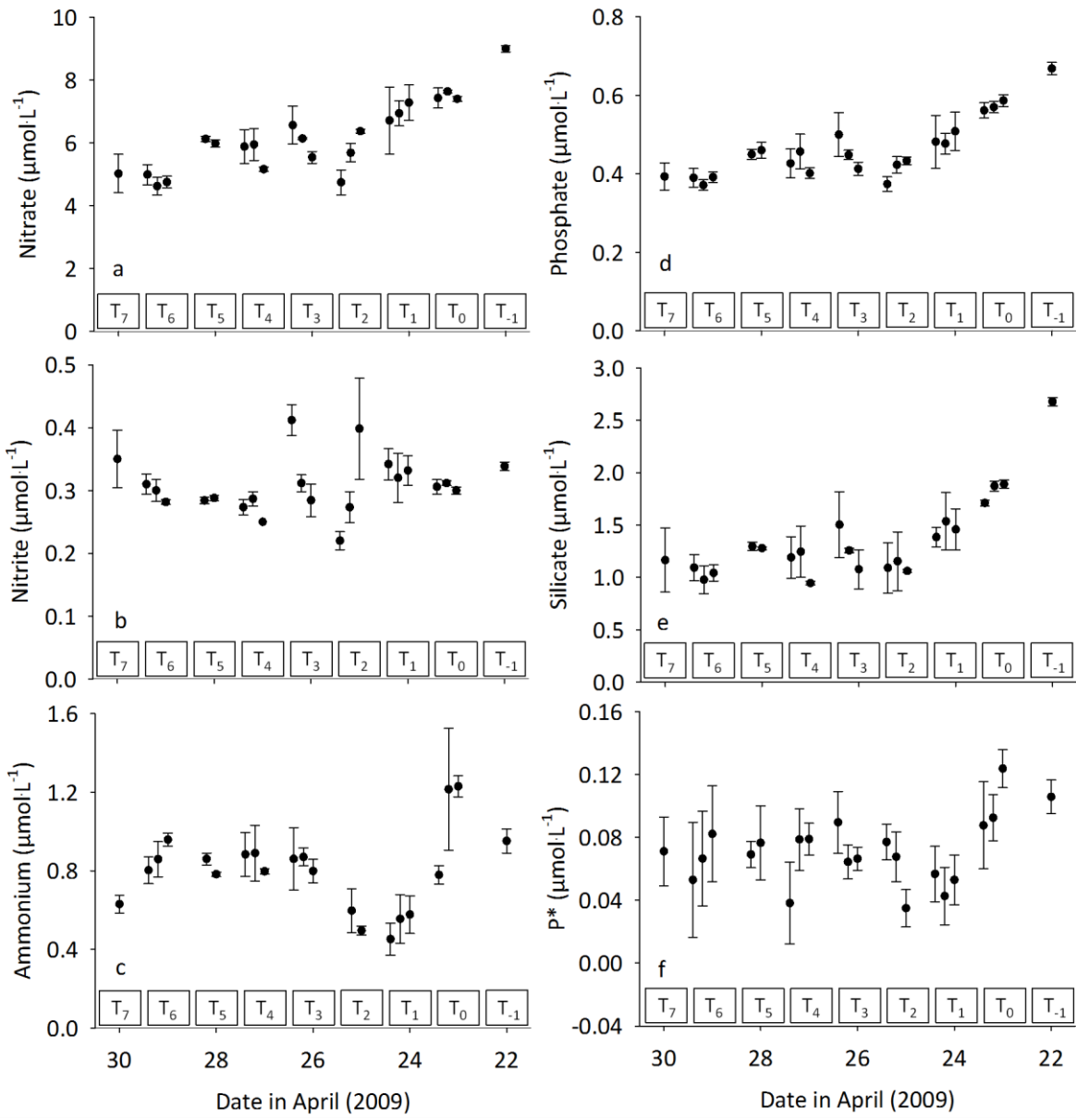
1 Fig. 1.

2



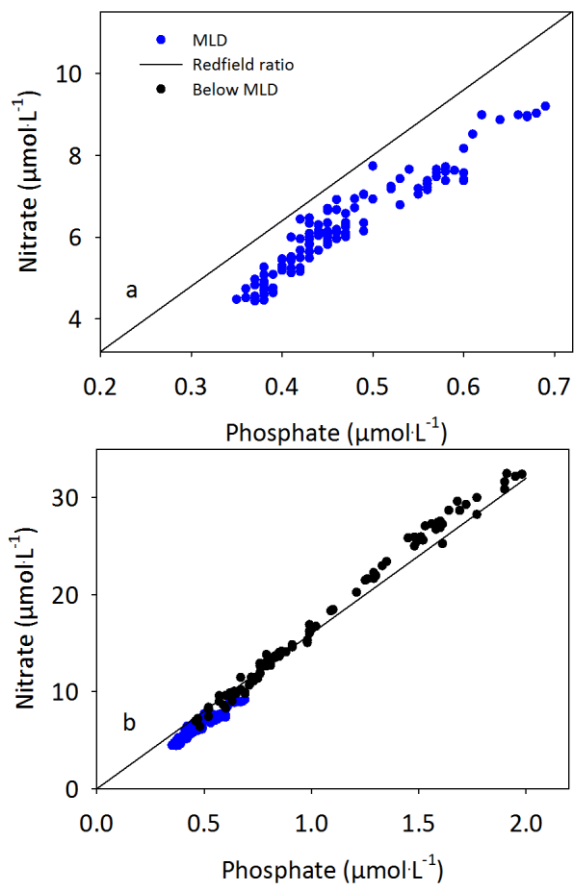
3  
4

1 Fig. 2



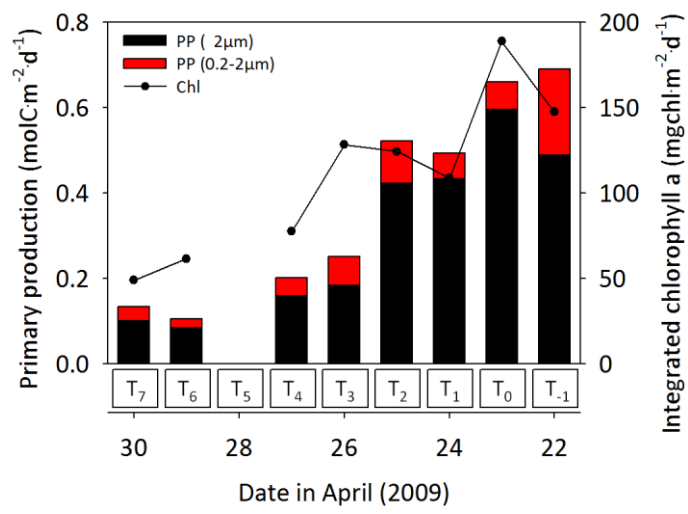
2  
3  
4  
5  
6  
7  
8  
9  
10  
11  
12  
13

1 Fig. 3



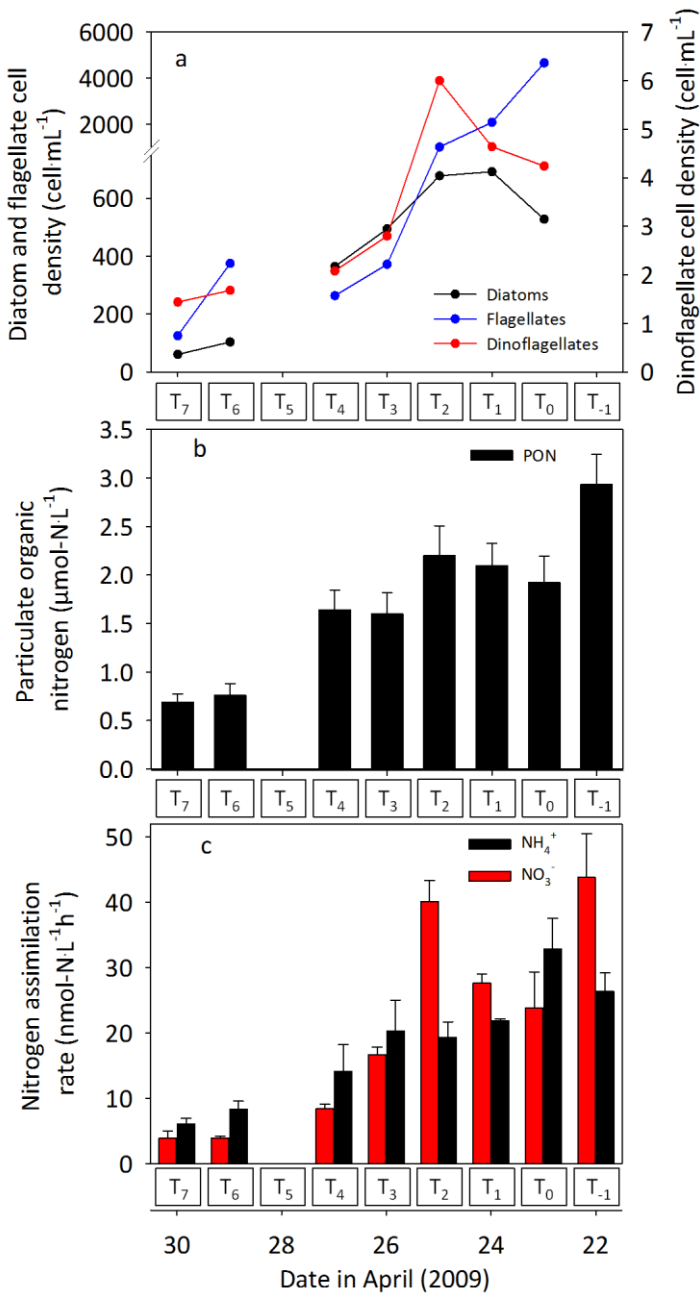
2  
3  
4

1 Fig. 4



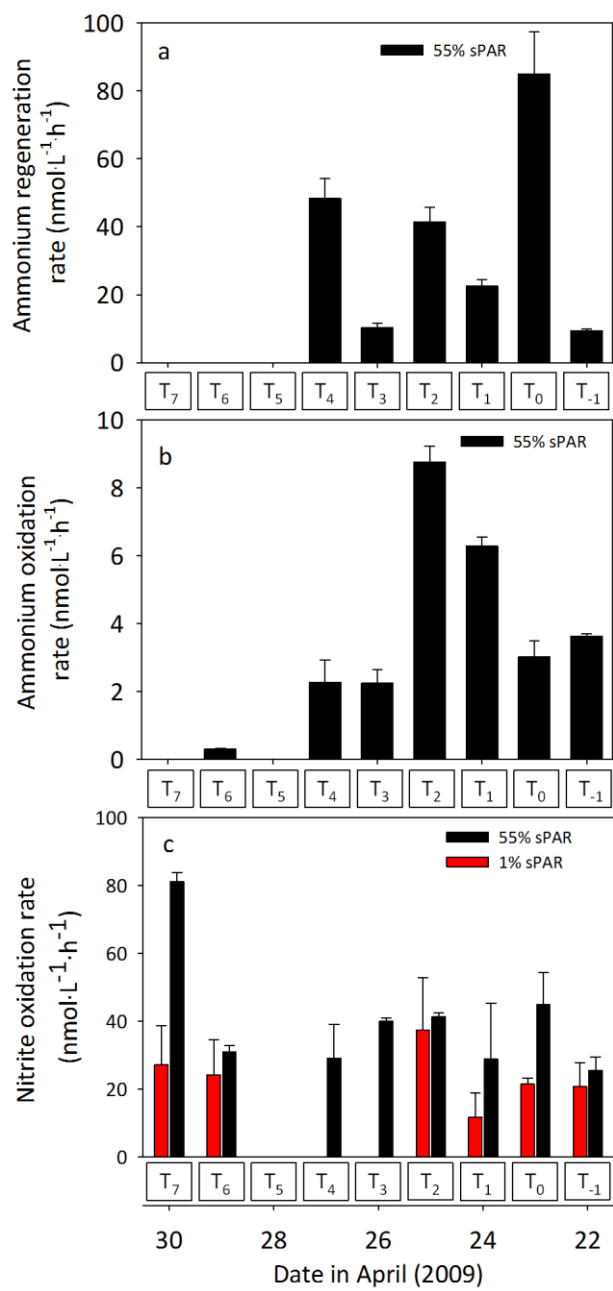
2

1 Fig. 5



2  
3  
4

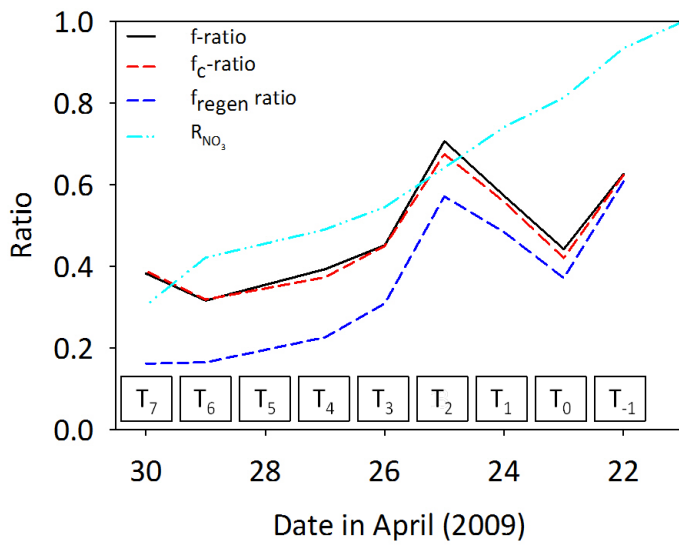
1 Fig. 6



2  
3  
4

1 Fig. 7

2



3